

Study of non-self-averaging on Polya's urn model using a perturbation analysis

野口, 慎平

<https://doi.org/10.15017/1931698>

出版情報 : 九州大学, 2017, 博士 (理学), 課程博士
バージョン :
権利関係 :

Study of non-self-averaging on Polya's urn model using a perturbation analysis

Shinpei Noguchi

Department of Physics
Kyushu University

Contents

1	Introduction	7
2	Self-averaging and non-self-averaging	11
2.1	The law of large numbers and two definitions of non-self-averaging . . .	11
2.2	Magnitude of Gross Domestic Product (GDP) in a simple model . . .	13
2.2.1	Model	13
2.2.2	Analysis of non-self-averaging	14
3	Urn models and their applications	17
3.1	The framework of an urn model	17
3.2	Distribution of growth rate of firms: Bottazzi-Secchi model	18
3.3	Bagchi and Pal model	20
3.4	Simon's urn model	22
3.5	Summary	23
4	Balanced Polya's urn and a perturbation analysis	25
4.1	Definition of balanced Polya's urn and its features	25
4.2	Monte Carlo simulation	26
4.2.1	Results of the simulations	27
4.3	Master equation of Polya's urn and its continuum approximation . . .	27
4.4	Non-self-averaging	32
4.5	Perturbation analysis	32
4.5.1	Response function	33
4.5.2	Relaxation function	34
4.5.3	Complex admittance	37
4.6	Conclusions	40
5	Non-linear Polya's urn model	45
5.1	Introduction	45
5.2	Definition of non-linear Polya's urn and the master equation	46

5.3	Non-self-averaging	47
5.4	Numerical example	50
5.4.1	Example 1	50
5.4.2	Example 2	52
5.5	Perturbation analysis	52
5.5.1	Example 3	57
5.5.2	Example 4	58
5.5.3	Classification of non-self-averaging	61
5.6	Conclusions	61
6	Conclusions	63

Abstract

The purpose of this thesis is to understand “non-self-averaging” phenomena. The definition of self-averaging is that a physical quantity divided by the system size is equal to its ensemble average. In particular, influences of non-self-averaging are investigated in time and frequency domains. To achieve this purpose, Polya’s urn model is examined because this model has been applied to many phenomena in the fields of physics, economics and biology. Polya’s urn model is a stochastic model consisting of white and black balls, where the numbers of white and black balls in the urn increase with time. This model has two parameters a and b that represent the amounts of the increases of the number of white and black balls at each step. When $a = b$ in this model, the process shows non-self-averaging. This thesis consists of two parts. First, I study (linear) Polya’s urn model by a perturbation analysis. Second, I investigate the properties of non-linear Polya’s urn.

In the first part, to study Polya’s urn model analytically, I employ the continuum approximation. I find a certain scaling law for the distribution of the number of black balls, and the obtained results agree with those obtained by Monte Carlo simulations. By a perturbation analysis, I find that the average of the reduced response function $\langle\phi(t, t - \tau)\rangle/t$ does not decay to 0 when self-averaging is violated.

In the second part, I investigate non-linear Polya’s urn model, where the probability of drawing a black ball is generalized by a non-linear function $Q(x_b)$. Here, the x_b is the fraction of black balls in the urn. I show that the steady distribution of x_b is given by $\sum_i \rho_i \delta(x_b - x_i^{st})$, where x_i^{st} ’s are the stable fixed points of the urn. The property of self-averaging is determined by the number of stable fixed points. Even if the process is non-self-averaging, the reduced response function for a finite number of x_i^{st} ’s vanishes in the long time limit. In contrast, the reduced response function for an infinite number of x_i^{st} ’s does not vanish in the long time limit. By these results, I propose that non-self-averaging has two classes.

Chapter 1

Introduction

Since Newton's laws of motion were established, physicists have attempted to explain the real world using the equations of motion and these plans have succeeded in natural science. Based on the basic physics laws, all physical phenomena can be predicted basically. In particular, some physicists or mathematicians (one of the most representative persons is Laplace) considered that all physical phenomena could be, in principle, investigated by solving the equations of motion. Thus, these scientists believed that thermodynamics explaining phenomena of macroscopic systems should be derived from the equations of motion.

However, in systems consisting of many particles whose number is typically 10^{23} , these attempts were impractical and unsuccessful. Macroscopic theories cannot be derived from microscopic theories such as the equations of motion. Different ideas were needed to connect microscopic equations of motion with macroscopic theories, such as thermodynamics.

One way of linking microscopic theories and macroscopic theories is through the law of large numbers in probability theories. Probability theories have been developed since the 17th century to choose wise strategies in gambles. In contrast to deterministic equations of motion, in probability theories, each microscopic physical quantity is regarded as a random variable $\sigma(i)$ where i labels a step in a certain stochastic process. Its value cannot be predicted for sure. However, by repeating many trials, a random variable $\mu = (1/N) \sum_i^N \sigma(i)$ is close to the average calculated by the distribution, where N is the number of steps. This statement is called the law of large numbers. It has been applied to the fields of gambling, insurance, etc., and guaranteed long-time benefits to its users even if they suffer damages in a short-time scale.

This application of probability theories is not limited to the discipline of mathematics and economics, and the idea of probability theories was introduced in physics

by Maxwell and Boltzmann at the end of the nineteenth century. To explain the nature of macroscopic systems Boltzmann replaced the many degrees of freedom in systems with a set of random variables. The motion of each element is probabilistic and unpredictable. However, in sufficiently large systems the fluctuations of each particle are canceled and the deterministic average value can be obtained. This idea is an application of the law of large numbers to physical systems.

The physics introduced by Boltzmann is called statistical physics today. In the early days, many physicists criticized his theory. However in the mid-20th century, statistical physics was accepted by the community of physicists as a theoretical tool to explain the behavior of the thermal equilibrium in a macroscopic system because the theory describes many properties of actual systems.

The applicability of such statistical ideas is not limited to physics. For example, financial theories can introduce such statistical ideas, because many people participate in a financial market. Statistical physics and financial theories based on the law of large numbers give us methods which explain macroscopic systems. For instance, the order-disorder transition and the price determination of insurance have been discussed in the framework of the law of large numbers.

In 1907, Markov had a question about the assumption on which the law of large numbers was based. The law of large numbers requires independence of each random variable. Even when this assumption does not hold, “the law of large numbers” does not always break. When this presupposition of independence is removed then, is the law of large numbers true in any stochastic processes[1]? This question is the first starting point of “non-self-averaging”. Markov’s argument is as follows: Consider N flips of a coin. When flips are independent, the law of large numbers is true. On the other hand, the law of large numbers does not necessarily hold when flips are correlated. By the degree of the correlation, the process shows “non-self-averaging” which means that the law of large numbers does not hold. One example in which the law of large numbers breaks down is that probability of heads of the coin is proportional to the number of heads in the previous flips.

In physics, Lifschitz firstly introduced the notion of “self-averaging”[2]. When the deviation of a particular physical quantity from the average vanishes as the system size goes to infinity (thermodynamic limit), the quantity is called self-averaging. Most of the extensive physical quantities are self-averaging in usual problems of statistical physics. However, in disordered systems such as spin glass systems[3], this property does not always hold.

In addition to the above insight by Lifschitz, Mandelbrot discovered “fractal” power-law distributions of prices in financial markets. Since many people participate in a financial market, the law of large numbers might be expected to hold there.

However, he showed that this naive expectation is violated; fractal distributions do not yield self-averaging.

Non-self-averaging has conventionally been studied on stationary systems[3, 4, 5, 6, 7, 8]. Non-self-averaging phenomena, however, emerge in time-evolving systems. Aoki introduced such examples in an economic growth model[9]. Modern economic theories are basically founded on the assumption of self-averaging. If economic growth is non-self-averaging, then today's economic policies are forced to be changed fundamentally. Hence it is important for us to understand non-self-averaging in the time domain.

In this thesis, I investigate the influence of non-self-averaging in time domain using Polya's urn model. Polya's urn model was introduced by Polya and Eggenberger in 1923[10]. This model is equivalent to that of Markov in 1907, and is the most popular in models exhibiting non-self-averaging. In addition, this simple model has wide applications in physics, biology, economics and graph theories. In order to study the above influence, I carry out a linear response analysis in Polya's urn model.

This thesis is organized as follows. Firstly, self-averaging and non-self-averaging are defined using the extension of the law of large numbers in Chapter 2. Using the definition, one can study non-self-averaging properties, by associating them with the fluctuations of a system. In Chapter 3, we review previous investigations and applications of Polya's urn model. These studies have shown that urn models play an important role in wide fields. In Chapter 4, I apply perturbations to Polya's urn model. The response functions, the relaxation functions and the complex admittances are studied by analytical calculations and Monte Carlo simulations. Next, in Chapter 5, I investigate the response of non-linear Polya's urn model to an applied perturbation by analytical calculations and Monte Carlo simulations. According to the results of this chapter, temporal properties of non-self-averaging can be classified into the following two types: the average of the response function divided by time decays to zero in one type, and it does not in the other. Finally, in Chapter 6, I give discussions and conclusions.

Chapter 2

Self-averaging and non-self-averaging

In this chapter, I give two definitions of non-self-averaging. For this purpose, I give a brief proof of the law of large numbers. The law of large numbers is the simplest case of self-averaging. By proving the law of large numbers, I show a relation between the variance and non-self-averaging. Finally, I explain stochastic processes having the property of non-self-averaging.

2.1 The law of large numbers and two definitions of non-self-averaging

The law of large numbers is a basic theorem in probability theories. This theorem plays an important role in systems consisting of many elements, and therefore guides statistical physics.

Consider a sequence of random variables x_1, \dots, x_N , where each variable follows independent and identical distributions $\{p(x_i)\}$. By using this notation, the average $\langle x_i \rangle$ and the variance $V(x_i)$ is defined by

$$\langle x_i \rangle = \int p(x_i)x_i dx_i, \quad (2.1)$$

and

$$V(x_i) = \int p(x_i)x_i^2 dx_i - \langle x_i \rangle^2, \quad (2.2)$$

respectively.

When x_i is independent and identically distributed, the law of large numbers is proved using Chebyshev's theorem: for an arbitrary random variable x , this

statement reads

$$P[|x - \langle x \rangle| \geq \sqrt{V(x)}k] \leq \frac{1}{k^2}, \quad (2.3)$$

where k is an arbitrary positive real number and $P[\text{event}]$ means the probability of occurring the event.

The law of large numbers:

The arithmetic average of N stochastic variables

$$x \equiv \frac{x_1 + x_2 + \cdots + x_N}{N} \quad (2.4)$$

and its ensemble average $\langle x \rangle$ obey

$$P[|x - \langle x \rangle| < \epsilon] \rightarrow 1 \quad (2.5)$$

in the limit of large N , where ϵ is an arbitrary positive real number.

The law of large numbers is proven as follows. Let us set $k = \epsilon/\sqrt{V(x)}$. Chebyshev's theorem is transformed as follows:

$$P[|x - \langle x \rangle| < \epsilon] \geq 1 - \frac{V(x)}{\epsilon^2}. \quad (2.6)$$

The variance $V(x)$ is

$$V(x) = \langle x^2 \rangle - \langle x \rangle^2 = \frac{v}{N}$$

where $v = \int p(x_i)x_i^2 dx_i - \langle x_i \rangle^2$. Note that v is independent of the index i because x_i 's obey identical distributions. In the limit of large N , the right hand side of eq. (2.6) converges to 1.

The law of large numbers holds when x_i 's are independent of each other. However, even if each x_i correlates, eq. (2.5) can be considered as the criterion applicable to any stochastic processes for the validity of the law of large numbers. With this in mind, one defines non-self-averaging as follows:

The definition of self-averaging

The $x(N)$ depending on the system size N is defined by the average

$$x(N) = \frac{x_1 + x_2 + \cdots + x_N}{N}. \quad (2.7)$$

Given the probability $p(x_1, x_2, \cdots, x_N)$, the ensemble average of $x(N)$ is denoted as $\langle x(N) \rangle$. When $P(|x(N) - \langle x(N) \rangle| < \epsilon) \rightarrow 1$ in the limit of $N \rightarrow \infty$, the sequence $\{x_i\}$ is called self-averaging. Otherwise this sequence is non-self-averaging.

According to Chebyshev's theorem, if the variance of $x(N)$ is 0 at $N \rightarrow \infty$, self-averaging holds and vice versa. From eq. (2.3), the probability $P[|x - \langle x \rangle| > \epsilon]$

tends to zero for any given positive ϵ when $V(x) \rightarrow 0$. In other words, we call $x(N)$ non-self-averaging if the variance of $x(N)$ does not converge to 0 ($V(x(N)) = \langle x(N)^2 \rangle - \langle x(N) \rangle^2 \neq 0$ as $N \rightarrow \infty$).

In some previous papers[12], non-self-averaging was defined in a different manner:

$$P[|x(N)/\langle x(N) \rangle - 1| < \epsilon] < 1 \quad (2.8)$$

in the limit of large N . Note that in above definition $x(N)$ is divided by the average of $x(N)$ instead of the system size N . This condition is equivalent to non-zero $CV(x)$ defined by

$$CV(x) = \lim_{N \rightarrow \infty} \frac{V(x(N))}{(\langle x(N) \rangle)^2} \quad (2.9)$$

In this thesis, my analysis adopt exclusively the former definition.

2.2 Magnitude of Gross Domestic Product (GDP) in a simple model

What actual phenomena exhibit non-self-averaging? Aoki studied an economic growth model to show that the self-averaging is violated in economic phenomena[11]. I review the study of Aoki in the field of economics in this subsection.

2.2.1 Model

I consider a simple model of economic growth. I particularly focus on the GDP. The number of industries at time t is K_t and the size of each industry i is represented by $n_i(t)$. At the initial time $t = 1$, let us set $K_1 = 1$ and $n_1(1) = 1$. At each time step, I assume that $\sum_{i=1}^{K_t} n_i$ increases by 1. Therefore, $\sum_{i=1}^{K_t} n_i = t$. The size of one of the industries is increased by 1 at each time step. Here, by using two parameters α, θ ($0 \leq \alpha < 1$ and $0 \leq \alpha + \theta$)¹, the probability of increasing the size of the i -th industry is given by

$$p_i = \frac{n_i(t) - \alpha}{t + \theta}. \quad (2.10)$$

The probability of creating a new industry is

$$1 - \sum_{i=1}^{K_t} p_i = \frac{\sum_{i=1}^{K_t} n_i(t) - K_t \alpha}{t + \theta} = \frac{\theta + K_t \alpha}{t + \theta}. \quad (2.11)$$

When the new industry is created, $K_{t+1} = K_t + 1$ and the K_{t+1} -th industry is newly defined as $n_{K_{t+1}}(t+1) = 1$.

¹The condition $0 \leq \alpha + \theta$ is required because the probability of eq.(2.11) must not be negative at any time.

2.2.2 Analysis of non-self-averaging

By using K_t and $n_i(t)$, Aoki defined the GDP as $Y(t) = \sum_{i=1}^{K_t} \gamma^{n_i(t)}$ where $\gamma \geq 1$. Now, is $Y(t)$ self-averaging? Aoki defined that $Y(t)$ is self-averaging when $\lim_{t \rightarrow \infty} CV(Y(t)) = 0$.

In the present thesis, the discussion is restricted to the case of $\gamma = 1$, where

$$Y(t) = K_t. \quad (2.12)$$

Here, I define the following random variables d_i :

$$d_i = \begin{cases} 1 & \text{when a new industry is created} \\ 0 & \text{otherwise,} \end{cases}$$

where i represents time. Thus,

$$\frac{Y(t)}{t} = \frac{K_t}{t} = 1 + \frac{\sum_{i=1}^t d_i}{t}. \quad (2.13)$$

This equation corresponds to eq. (2.7). Therefore, I only need to consider $CV(Y(t))$ because $CV(Y(t)) = CV(Y(t)/t)$.

The distribution of $k = K_t$ is represented by $P(k, t)$, and I can obtain the master equation

$$P(k, t+1) = \frac{\theta + \alpha(k-1)}{\theta + t} P(k-1, t) + \left\{ 1 - \frac{\theta + \alpha k}{\theta + t} \right\} P(k, t) \quad (2.14)$$

where the first term in the right hand side represents the probability of creating a new industry at time t , and the second term represents the probability that a new industry is not created at time t . When $t \gg 1$, and $k \gg 1$, the master equation can be approximated as

$$\frac{\partial P(k, t)}{\partial t} = -\frac{\partial}{\partial k} \left\{ \frac{\theta + \alpha k}{\theta + t} P(k, t) \right\}. \quad (2.15)$$

From eq. (2.15), I have

$$\begin{aligned} \frac{d\langle K_t \rangle}{dt} &= \frac{\theta + \alpha \langle K_t \rangle}{\theta + t} \\ &\simeq \frac{\theta + \alpha \langle K_t \rangle}{t}. \end{aligned} \quad (2.16)$$

The solution is given by

$$\langle K_t \rangle = \frac{(\alpha + \theta)t^\alpha - \theta}{\alpha}. \quad (2.17)$$

Note that the initial condition is given by $K_1 = 1$.

Likewise, the differential equation for the average of K_t^2 is

$$\begin{aligned}\frac{d\langle K_t^2 \rangle}{dt} &= 2\frac{\theta\langle K_t \rangle + \alpha\langle K_t^2 \rangle}{\theta + t} \\ &\simeq 2\frac{\theta\langle K_t \rangle + \alpha\langle K_t^2 \rangle}{t}.\end{aligned}\quad (2.18)$$

From eqs. (2.16) and (2.18), the variance of K_t must satisfy the following differential equation

$$\begin{aligned}\frac{dV(K_t)}{dt} &= \frac{d\langle K_t^2 \rangle}{dt} - 2\langle K_t \rangle \frac{d\langle K_t \rangle}{dt} \\ &= 2\frac{\alpha V(K_t)}{t}.\end{aligned}\quad (2.19)$$

Thus, $V(K_t) \propto t^{2\alpha}$, and $CV(K_t)$ defined by

$$CV(K_t) = \frac{V(K_t)}{\langle K_t \rangle^2} \quad (2.20)$$

is proportional to

$$\frac{\alpha t^\alpha}{(\alpha + \theta)t^\alpha - \theta}. \quad (2.21)$$

Therefore, $\lim_{t \rightarrow \infty} CV(K_t) \neq 0$ when $0 < \alpha < 1$. If $\lim_{t \rightarrow \infty} CV(K_t)$ at $\alpha = 0$ is defined by $\lim_{\alpha \rightarrow 0} \lim_{t \rightarrow \infty} CV(K_t)$, then $\lim_{t \rightarrow \infty} CV(K_t) = 0$ at $\alpha = 0$. Consequently, K_t is non-self-averaging (self-averaging) for $0 < \alpha < 1$ ($\alpha = 0$).

By using eq. (2.12), one can show that the relative variance $CV(Y(t))$ does not go to 0 unless $\alpha = 0$. A random variable Nx_i in eq. (2.7) corresponds to d_i . Finally, from the definition of non-self-averaging of Aoki, one can find that $Y(t)$ is non-self-averaging when $\alpha \neq 0$.

This result can be understood intuitively as follows. The probability of creating a new industry is

$$1 - \sum_{i=1}^{K_t} p_i = \frac{\theta + \alpha K_{t-1}}{\theta + t}. \quad (2.22)$$

When $\alpha = 0$, this probability is

$$\frac{\theta}{\theta + t} \quad (2.23)$$

and does not depend on K_{t-1} . The correlation between $\Delta K_t = K_t - K_{t-1}$ and $\Delta K_{t-1} = K_{t-1} - K_{t-2}$ does not exist. This means that K_t does not depend on the previous history of the system. Therefore, self-averaging holds. In contrast, for $\alpha \neq 0$, the probability given by eq. (2.22) includes K_{t-1} . Since K_t depends on the previous number of industries, the correlation between K_t and K_{t-1} exists. Therefore, for $\alpha \neq 0$, self-averaging can be violated.

Chapter 3

Urn models and their applications

As mentioned in the previous chapter, phenomena exhibiting non-self-averaging emerge in a variety of fields. However, the properties of non-self-averaging in the time domain are not sufficiently understood. Analysis of these properties in a general framework is difficult. I limit the subject of my study to stochastic urn models.

Urn models are simple stochastic models and are easy to analyze. Moreover, it is surprising that urn models can describe phenomena in many fields[14, 15, 16, 17]. In this chapter, I review some applications of urn models.

3.1 The framework of an urn model

Urn models basically consist of colored balls and an urn[18]. The state of the urn at time t is represented by a set of the number of each colored ball:

$$\mathbf{n}(t) = (n_1(t), n_2(t), \dots, n_K(t)) \quad (3.1)$$

where K denotes the number of colors, and $n_i(t)$ represents the number of the balls of color i at time t . The initial state of the urn is

$$\mathbf{n}(0) = (n_1(0), n_2(0), \dots, n_K(0)). \quad (3.2)$$

At time t , the urn's state is determined by the following recursive processes: (1) One draws a ball from the urn at time $t - 1$ and the probability that the color of the ball is i is the fraction of balls of color i in the urn. (2) Check the color of the ball, and if this color is i , urn's state $\mathbf{n}(t)$ is given by

$$\mathbf{n}(t) = (n_1(t-1) + a_{i1}, n_2(t-1) + a_{i2}, \dots, n_K(t-1) + a_{iK}) \quad (3.3)$$

where (a_{ij}) is called the matrix of the urn, and its elements are integers.

When all a_{ij} 's are non-negative, this model is called Polya's urn model. For Polya's urn, the number of colors K is assumed to be constant. In some models, one assumes that K increases stochastically. As such models, Simon's urn model and Hoppe's urn model are well known. These two models obey similar rules. At the end of this chapter, I explain Simon's urn.

3.2 Distribution of growth rate of firms: Bottazzi-Secchi model

Amaral *et al.* (2001) discovered that the distribution of the growth rate g of a firm follows the Laplace distribution[19]. Here, the growth rate is defined by

$$g = \frac{S_{t+1} - S_t}{S_t}, \quad (3.4)$$

where S_t is the size of the firm at time t , and the firm size is measured by the cost of goods sold or a sales volume. When g is small, the above equation can be approximated¹ by

$$g \simeq \ln S_{t+1} - \ln S_t. \quad (3.5)$$

The Laplace distribution $P_L(g)$ is

$$P_L(g) = \frac{1}{2\sigma} \exp\left(-\frac{|g - \mu|}{\sigma}\right), \quad (3.6)$$

where μ is the average of g , and $2\sigma^2$ is the variance of g .

Bottazzi and Secchi proposed a model of Polya's urn in order to explain the observation of Amaral *et al.*[20] First, they assumed that each firm i has a value of "business opportunities", which is a positive integer given by a stochastic process. A firm size is determined by the business opportunities. If the size and business opportunity of a firm i at time $t - 1$ are S_{t-1}^i and $n_i(t - 1)$, respectively, the size at time t , S_t^i , is assumed to be calculated by

$$\ln S_t^i = \ln S_{t-1}^i + \sum_{j=1}^{n_i(t-1)} \epsilon_j, \quad (3.7)$$

where ϵ_j is a random variable following the normal distribution with the average being 0, and the variance being v .

Next, $n_i(t)$ is assumed to obey Polya's urn model whose matrix is $(a_{ij}) = (\delta_{ij})$. A firm i corresponds to color i of Polya's urn model. An initial state is set to

$$\mathbf{n}(0) = (1, 1, \dots, 1). \quad (3.8)$$

¹When $\Delta x \ll 1$, the formula $\ln(1 + \Delta x) \simeq \Delta x$ holds for $O(\Delta x)$

By using Polya's urn processes, business opportunities of firm i are obtained as the number of balls of color i , $n_i(t)$.

Under these assumptions, from eqs. (3.4) and (3.5), the growth rate $g_i(t)$ is determined by

$$g_i(t) = \sum_{j=1}^{n_i(t)} \epsilon_j. \quad (3.9)$$

Bottazzi and Secchi showed that the growth rate $g_i(t)$ obtained by the method presented above obeys the Laplace distribution.

To prove this, let us consider the probability $P_N(n, t)$ that the business opportunity of a given firm is n at time t when the number of firms is N . The total number of drawing from the urn is t and the given firm is chosen $n - 1$ times. At the initial time $t = 0$, $n(0) = 1$ and the number of the other firms is $N - 1$. First, I consider the special order of the choices that the given firm is chosen $n - 1$ times in a row before the other firms are chosen $t - n + 1$ times. This probability is given by

$$\frac{(n-1)!(N-1) \cdot N \cdots (N+t-n-1)}{N \cdot (N+1) \cdots (N+t-1)}. \quad (3.10)$$

Next, I consider the probability of choosing the firms at an arbitrary order $P_N(n, t)$. The probability of a certain order is equal to eq. (3.10) [21]. Therefore, $P_N(n, t)$ is eq. (3.10) multiplied by combination ${}_t C_{n-1}$. Hence, I obtain

$$P_N(n, t) = \frac{(n-1)!(N-1) \cdot N \cdots (N+t-n-1)}{N \cdot (N+1) \cdots (N+t-1)} {}_t C_{n-1} \quad (3.11)$$

$$= \frac{\Gamma(N+t-n-1)\Gamma(t)\Gamma(N-1)}{\Gamma(N-2)\Gamma(N+t-1)\Gamma(t-n+1)}, \quad (3.12)$$

where $\Gamma(x)$ is the gamma function. Let us set $\lambda = t/N$. When $N \gg 1$, and $t \gg 1$, using the formula $\Gamma(x+a)/\Gamma(x) \sim x^a$ for $x \gg 1$, eq. (3.12) is approximated as

$$P_N(n, t) \sim \frac{\lambda^{n-1}}{(1+\lambda)^n}. \quad (3.13)$$

Thus the distribution of the growth rate g is given by

$$f_N(g, t) = \sum_{n=1}^t P_N(n, t) \left(\frac{1}{\sqrt{2\pi v}} \right)^n \prod_{i=1}^n \int_{-\infty}^{\infty} dg_i \delta\left(\sum_{j=1}^n g_j - g\right) \exp\left[-\frac{g_i^2}{2v}\right]. \quad (3.14)$$

The characteristic function of $f_n(g, t)$ is defined by

$$\hat{f}_N(h, t) = \int_{-\infty}^{\infty} dg \exp[-ihg] f_N(g, t). \quad (3.15)$$

As $t \rightarrow \infty$, $N \rightarrow \infty$ with λ fixed,

$$\hat{f}(h, \lambda) \stackrel{\text{def}}{=} \lim_{t \rightarrow \infty, \lambda = \text{const.}} \hat{f}_N(h, t) \quad (3.16)$$

$$\begin{aligned} &\simeq \frac{1}{1 + \lambda} \sum_{n=1}^{\infty} \left(\frac{\lambda}{1 + \lambda} \right)^{n-1} \exp \left[-\frac{vh^2}{2\lambda} \right]^n \\ &= \frac{\exp \left[-\frac{vh^2}{2\lambda} \right]}{1 + \lambda - \lambda \exp \left[-\frac{vh^2}{2\lambda} \right]}. \end{aligned} \quad (3.17)$$

If $\lambda \gg 1$ ($N \gg t$),

$$\hat{f}(h, \lambda) \simeq \frac{1}{1 + \frac{vh^2}{2}} + O \left(\frac{1}{\lambda} \right). \quad (3.18)$$

The above characteristic function is the same as that of the Laplace distribution with the average being 0, and the variance being $\sqrt{v/2}$ in the limit $\lambda \rightarrow \infty$. Q.E.D.

3.3 Bagchi and Pal model

Bagchi and Pal studied the asymptotic behavior of $n_1(t)$ in Polya's urn model when $K = 2$ and $a_{11} + a_{12} = a_{21} + a_{22} = b$ [22]. They demonstrated that the distribution of the random variable

$$z(t) = \frac{n_1(t) - \langle n_1(t) \rangle}{\sqrt{\langle n_1(t)^2 \rangle - \langle n_1(t) \rangle^2}} \quad (3.19)$$

converges to the normal distribution with the average being 0, and the variance being 1 in the long time limit.

Their proof is obtained by the calculations of the r -th moment of $z(t)$. Now, it is clear that two basic relations

$$P[n_1(t+1) = n_1(t) + a_{11} \mid n_1(t)] = \frac{n_1(t)}{n_1(0) + n_2(0) + bt} \quad (3.20)$$

$$P[n_1(t+1) = n_1(t) + a_{21} \mid n_1(t)] = 1 - \frac{n_1(t)}{n_1(0) + n_2(0) + bt} \quad (3.21)$$

hold, where $P[x|y]$ represents the probability of x for given y . Note that the total number of balls at t is $n_1(0) + n_2(0) + bt$. Here, they defined $y_1(t)$ as

$$y_1(t) = n_1(t) - (n_1(0) + n_2(0) + bt) \frac{a_{21}}{a_{12} + a_{21}}. \quad (3.22)$$

By using eq. (3.22), $z(t)$ is rewritten as

$$z(t) = \frac{y_1(t) - \langle y_1(t) \rangle}{\sqrt{\langle y_1(t)^2 \rangle - \langle y_1(t) \rangle^2}}. \quad (3.23)$$

To calculate an arbitrary moment of $z(t)$, the conditional average $\langle x \rangle_y$ is defined as

$$\langle x \rangle_y = \int xP[x|y]dx. \quad (3.24)$$

From eqs. (3.20) and (3.21),

$$\begin{aligned} & \langle y_1^r(t+1) \rangle_{y_1(t)} \\ &= \left(y_1(t) + a_{11} - a_{21} \frac{a_{11} + a_{12}}{a_{12} + a_{21}} \right)^r \left(\frac{a_{21}}{a_{12} + a_{21}} + \frac{y_1(t)}{n_1(0) + n_2(0) + bt} \right) \\ &+ \left(y_1(t) + a_{21} - a_{21} \frac{a_{11} + a_{12}}{a_{12} + a_{21}} \right)^r \left(\frac{a_{12}}{a_{12} + a_{21}} - \frac{y_1(t)}{n_1(0) + n_2(0) + bt} \right) \end{aligned} \quad (3.25)$$

where r is a natural number. Averaging eq. (3.25) with respect to $y_1(t)$, they obtained

$$\begin{aligned} \langle y_1^r(t+1) \rangle &= \left(1 + r \frac{a_{11} - a_{21}}{n_1(0) + n_2(0) + bt} \right) \langle y_1^r(t) \rangle \\ &= \sum_{i=1}^r \left(p_{r,r-i} + \frac{q_{r,r-i}}{n_1(0) + n_2(0) + bt} \right) \langle y_1^{r-i}(t) \rangle, \end{aligned} \quad (3.26)$$

where

$$p_{r,r-i} = {}_r C_i \left(\frac{a_{11} - a_{21}}{a_{12} + a_{21}} \right)^i \frac{a_{12}a_{21}}{a_{12} + a_{21}} [a_{12}^{i-1} + (-1)^i a_{21}^{i-1}] \quad (3.27)$$

$$q_{r,r-i} = {}_r C_{i+1} \left(\frac{a_{11} - a_{21}}{a_{12} + a_{21}} \right)^{i+1} [a_{12}^{i+1} + (-1)^i a_{21}^{i+1}]. \quad (3.28)$$

Solving eq. (3.26), for even $r \geq 2$, they found

$$\langle y_1^r(t) \rangle = 1 \cdot 3 \cdots (r-1) E^{r/2} (n_1(0) + n_2(0) + bt)^{r/2} + o(t^{r/2}) \quad (3.29)$$

where

$$E = \frac{a_{12}a_{21}(a_{11} - a_{21})^2}{(a_{12} + a_{21})^2(a_{11} - 2a_{12} - 2a_{21})}. \quad (3.30)$$

On the other hand, when r is odd,

$$\langle y_1^r(t) \rangle = o(t^{r/2}). \quad (3.31)$$

From eqs. (3.29) and (3.31), all the arbitrary moments of $z(t)$ in the long time limit are calculated as

$$\lim_{t \rightarrow \infty} \langle z(t)^r \rangle = \begin{cases} 1 \cdot 3 \cdots (r-1) & (\text{for even } r) \\ 0 & (\text{otherwise}). \end{cases} \quad (3.32)$$

Note that $\langle z(t) \rangle = 0$. Recall that the r -th moment of the normal distribution with the average being 0 and the variance being 1 is the same as that given by eq. (3.32). Because all the arbitrary moments agree with those of the normal distribution, $z(t)$ converges to the normal distribution in the limit $t \rightarrow \infty$.

3.4 Simon's urn model

In contrast to the above models, K of Simon's urn model increases stochastically. Simon's urn is proposed by Simon [23] to explain the origin of Zipf's law:

Zipf's law

Let k_i denote the frequency of the i -th most frequent events. Then, Zipf's law states that

$$k_i \propto \frac{1}{i}. \quad (3.33)$$

If $C(k_i > k)$ is defined as the number of the types of events whose frequency is larger than k , from eq. (3.33), one can obtain

$$C(k_i > k) \propto \frac{1}{k}. \quad (3.34)$$

Zipf's law was observed by a linguist Zipf in the 20th century, and holds in a wide variety of data sets, such as the frequency of words in a book, the size of cities in U. S. A., the magnitude of earthquakes, and chess openings.

In Simon's urn, there is only one ball at the initial time. At time t , with probability α ($0 \leq \alpha \leq 1$) one adds a new color ball in the urn. The new color means that this color differs from those of other balls contained in the urn up to time $t - 1$. When the event of adding a new color ball occurs,

$$K(t + 1) = K(t) + 1, \quad (3.35)$$

where $K(t)$ represents the number of colors at time t . The initial condition is given by $K(1) = 1$. With probability $1 - \alpha$, a ball is added under the rule of Polya's urn with $a_{ij} = \delta_{ij}$ (see Section 3.1). Here, α is a model parameter.

To investigate the distribution of the number of balls of new color that appear for the first time at time k , one can consider the following master equation:

$$P_k(n, t + 1) = (1 - \alpha) \left\{ \frac{n - 1}{1 + t} P_k(n - 1, t) + \left(1 - \frac{n}{1 + t} \right) P_k(n, t) \right\} + \alpha P_k(n, t) \quad (3.36)$$

where $P_k(n, t)$ is the distribution of n at time t , and n is the number of balls of that color. As time increases, $P_k(n, t)/t$ converges to a stationary distribution as long as $t > k$.

Now I derive Zipf's law from eq. (3.36). When $n \gg 1$, and $t \gg 1$, eq. (3.36) is regarded as a differential equation

$$\frac{\partial P_k(n, t)}{\partial t} = -\frac{1 - \alpha}{t} \frac{\partial}{\partial n} \{nP_k(n, t)\}. \quad (3.37)$$

To solve the above equation, I assume the following form:

$$P_k(n, t) = F_k(n)t. \quad (3.38)$$

Substituting $F_k(n)t$ for $P_k(n, t)$, I obtain

$$F_k(n) = -(1 - \alpha) \frac{d}{dn} \{nF_k(n)\}. \quad (3.39)$$

The equation (3.39) becomes

$$\frac{dF}{F_k(n)} = \frac{dn}{\left(-1 - \frac{1}{1-\alpha}\right)n}. \quad (3.40)$$

Thus, I have

$$F_k(n) \propto n^{-1 - \frac{1}{1-\alpha}} \quad (3.41)$$

in the long time limit. If $\alpha \ll 1$, $F_k(n) \propto n^{-2}$, and the cumulative distribution function $C(n > k)$ is given by

$$C(n > k) = \int_k^\infty n^{-2} dn = k^{-1}. \quad (3.42)$$

This distribution obeys a power-law of the exponent -1 , and exhibits Zipf's law.

3.5 Summary

In the previous investigations of Polya's urn, researchers have studied mainly asymptotic behaviors in the long time limit[22, 24]. According to these papers, Polya's urn has the property of non-self-averaging in a certain region of parameters. However, non-self-averaging phenomena can be observed in the short time range as well as in the asymptotic behaviors. Non-self-averaging phenomena in such short time range have not been studied yet. Therefore, in the next chapter I study short-time behavior of non-self-averaging by dealing mainly with perturbed Polya's urn processes. By investigating the perturbation of the process, I relate the property of non-self-averaging to the response to the perturbation.

Chapter 4

Balanced Polya's urn and a perturbation analysis

In Chapter 3, I introduced the urn models and showed their features. In this chapter, the number of colors in the model treated is limited to two. Our model is equivalent to setting $K = 2$ in eq. (3.1) and (a_{ij}) is a 2×2 matrix.

4.1 Definition of balanced Polya's urn and its features

Polya's urn with $K = 2$ is a stochastic model defined by two variables $\{n_a(t), n_b(t)\}$ and characterized by non-negative four parameters $(\alpha, \beta, \gamma, \delta)$. The two variables $n_a(t)$ and $n_b(t)$ represent the states of Polya's urn and evolve according to stochastic processes represented by the following equations:

$$\begin{aligned}n_a(t+1) &= n_a(t) + \alpha\sigma_t + \gamma(1 - \sigma_t) \\n_b(t+1) &= n_b(t) + \beta\sigma_t + \delta(1 - \sigma_t),\end{aligned}\tag{4.1}$$

where σ_t is a random variable taking either 0 or 1. Here, the probability of $\sigma_t = 0$ ($\sigma_t = 1$) is proportional to $n_a(t)$ ($n_b(t)$). The initial state of the urn at $t = 1$ is set as $n_a(1) = n_b(1) = 1$. In the following, the two variables $\{n_a, n_b\}$ are considered to represent the numbers of white balls and black balls, respectively.

When the four parameters $\alpha, \beta, \gamma, \delta$ satisfy

$$\alpha + \beta = \gamma + \delta,\tag{4.2}$$

this model is referred to as balanced Polya's urn. Furthermore, I choose the following

specific parameters

$$\alpha = b \quad (4.3)$$

$$\beta = 0 \quad (4.4)$$

$$\gamma = b - a \quad (4.5)$$

$$\delta = a. \quad (4.6)$$

In this case, the whole number of balls is

$$N(t) \equiv n_a(t) + n_b(t) = 2 + b(t - 1). \quad (4.7)$$

From (4.1), one obtains

$$n_b(t) = 1 + a \sum_{i=1}^t (1 - \sigma_i). \quad (4.8)$$

Therefore, the number of black balls $n_b(t)$ is represented by the summation of many stochastic variables σ_i . In contrast to the case where the law of large numbers holds, σ_i is not independent or identically distributed.

4.2 Monte Carlo simulation

In this section, the distribution of n_b at time t is obtained by numerical calculations [25], whose method is as follows:

Monte Carlo method:

Here I explain this method for an urn with white balls and black balls. Let the initial numbers of white and black balls be $n_a(1) = n_b(1) = 1$. Suppose that at Monte Carlo step t , the numbers of white and black balls are $n_a(t)$ and $n_b(t)$, respectively. Time development is defined by the following recursive procedure. If a white ball is drawn (this probability is $n_a(t)/(n_a(t) + n_b(t))$), then

$$\begin{aligned} n_a(t+1) &= n_a(t) + b \\ n_b(t+1) &= n_b(t). \end{aligned} \quad (4.9)$$

If a black ball is drawn (this probability is $1 - n_a(t)/(n_a(t) + n_b(t)) = n_b(t)/(n_a(t) + n_b(t))$), then

$$\begin{aligned} n_a(t+1) &= n_a(t) + b - a \\ n_b(t+1) &= n_b(t) + a. \end{aligned} \quad (4.10)$$

The distribution of the number of black balls n_b at time t , $P(n_b, t)$, is calculated by the iterations of the above processes.

4.2.1 Results of the simulations

To obtain $P(n_b, t)$, the number of black balls $n_b(t)$ recorded in each simulation is summed over all samples and divided by the sample number, 10^6 .

Figure 4.1 shows $P(n_b, t)$ at $t = 10, 20, 30, 40$, and 50 when $a = b = 1$. The distributions are flat and become broader as time increases. Figure 4.2 shows $P(n_b, t)$ at $t = 10, 20, 30, 40$, and 50 when $a \neq b$. The distributions have a well-defined maximum with a rapidly decaying tail in contrast to the previous case, and become broader with increasing time.

4.3 Master equation of Polya's urn and its continuum approximation

In this section, a master equation is considered in order to obtain an analytical solution of the distribution for Polya's urn model [25]. To determine $P(n_b, t)$, one can derive the master equation from eq. (4.9) and eq. (4.10):

$$P(n_b, t + 1) = \frac{n_b - a}{N(t)} P(n_b - a, t) + \frac{N(t) - n_b}{N(t)} P(n_b, t). \quad (4.11)$$

Since it is difficult to solve this discrete equation, I employ the continuous variable approximation of eq. (4.11). When $t \gg 1$, and $n_a \gg a$, one can obtain

$$P(n_b, t + 1) \simeq P(n_b, t) + \frac{\partial P(n_b, t)}{\partial t}, \quad (4.12)$$

and

$$\frac{n_b - a}{N(t)} P(n_b - a, t) + \frac{N(t) - n_b}{N(t)} P(n_b, t) \simeq P(n_b, t) - \frac{a}{bt} \frac{\partial [n_b P(n_b, t)]}{\partial n_b}. \quad (4.13)$$

Thus the master equation in the continuum approximation is

$$\frac{\partial P(n_b, t)}{\partial t} = -\frac{a}{bt} \frac{\partial [n_b P(n_b, t)]}{\partial n_b}. \quad (4.14)$$

A general solution to this partial differential equation (PDE) is obtained by

$$P(n_b, t) = t^{-a/b} f(n_b/t^{a/b}), \quad (4.15)$$

where $f(x)$ is a non-negative arbitrary differentiable function.

As shown in Figs. 4.3 and 4.4, scaling laws hold. The results obtained by the simulations show that scaled distributions $t^{a/b} P(n_b, t)$ at $t = 10, 30$ and 50 are represented by one curve $f(n_b/t^{a/b})$. This shows that the continuum approximation is valid.

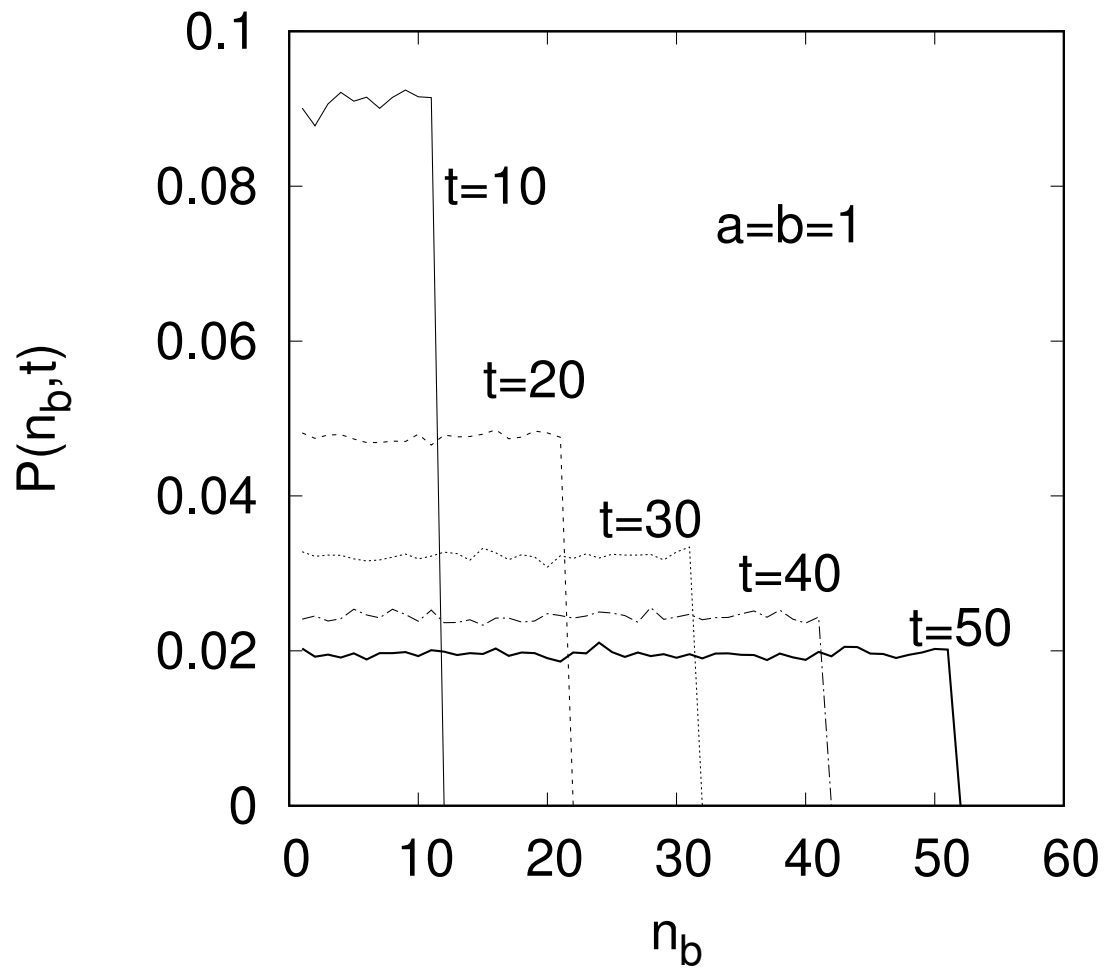


Figure 4.1: The distribution function $P(n_b, t)$ as a function of n_b at $t = 10, 20, 30, 40,$ and 50 for $a = b = 1$.

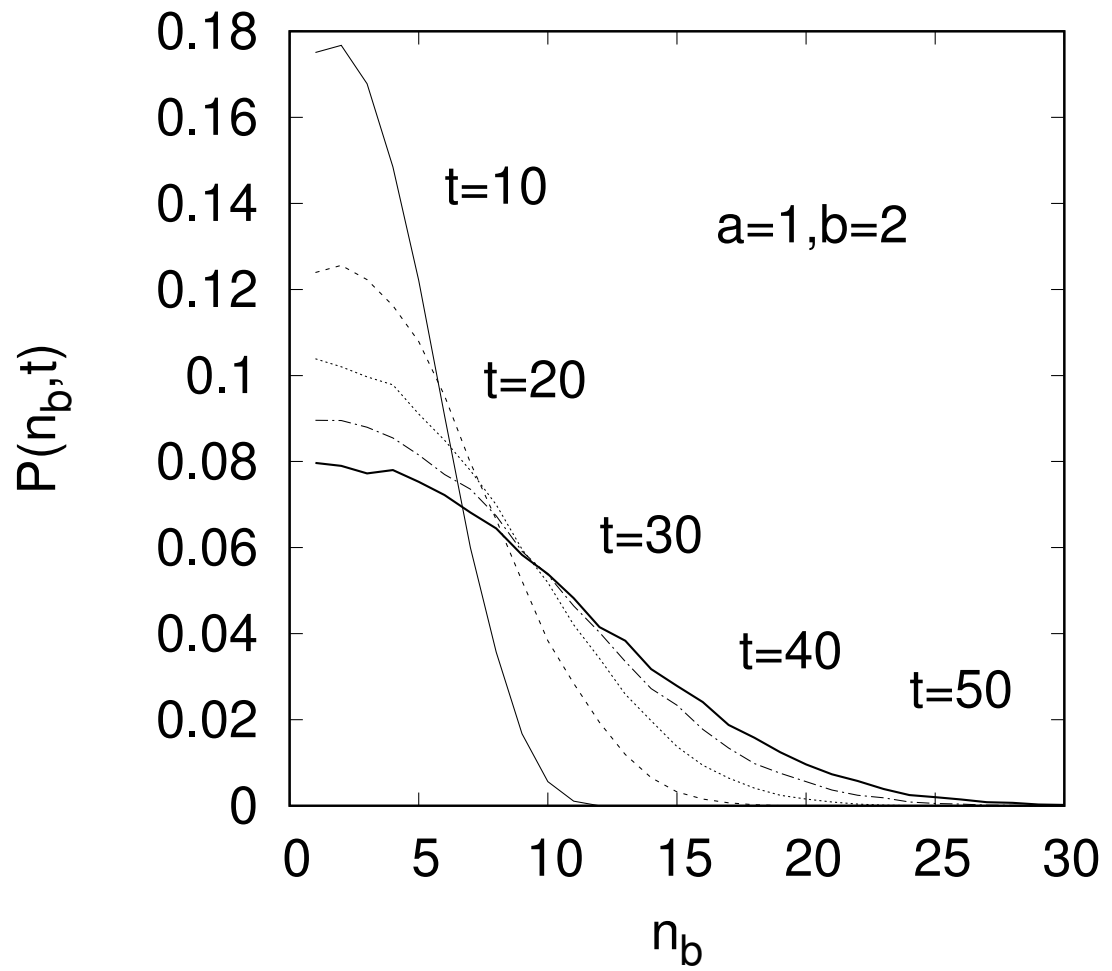


Figure 4.2: The distribution function $P(n_b, t)$ as a function of n_b at $t = 10, 20, 30, 40,$ and 50 for $a = 1$ and $b = 2$.

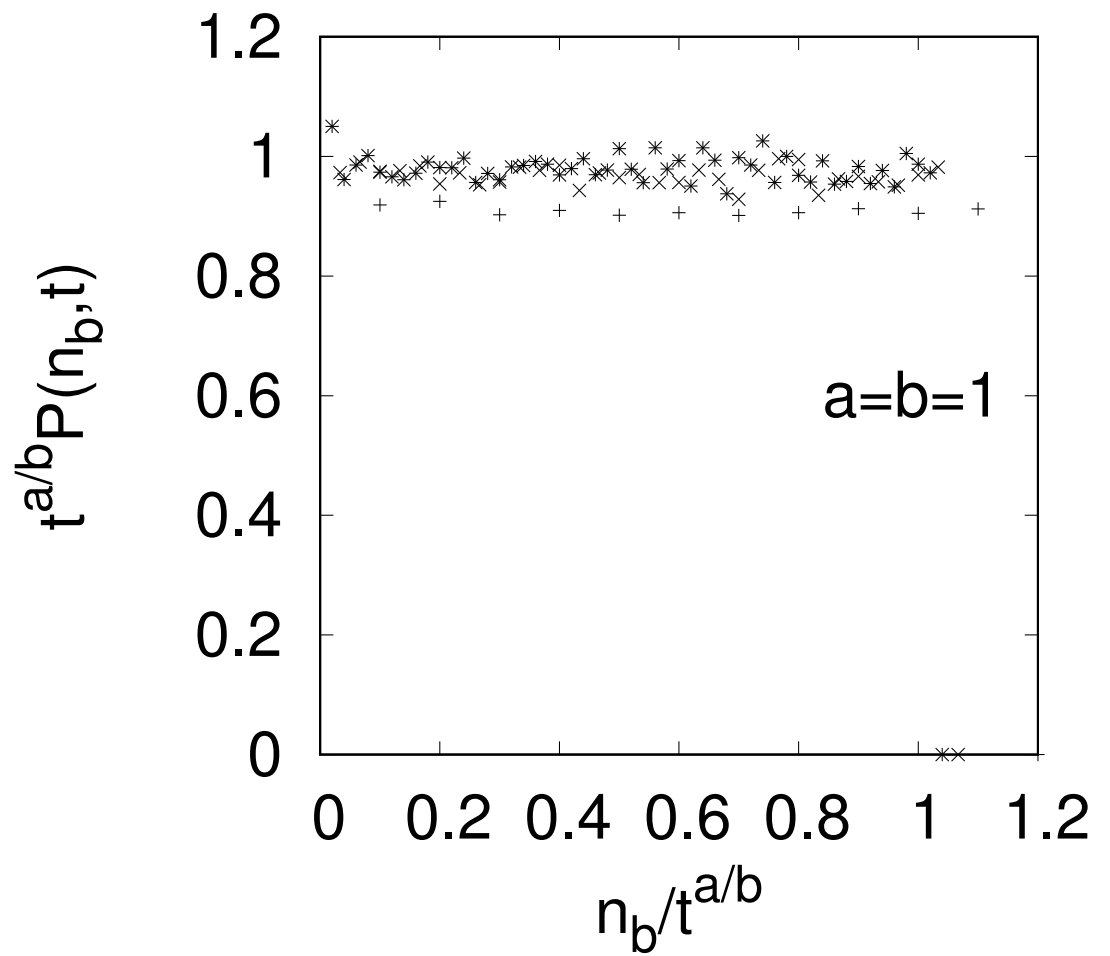


Figure 4.3: The scaled probabilities $t^{a/b}P(n_b, t)$ obtained by the same data as fig. 4.1 at $t = 10(+)$, $30(x)$, and $50(*)$ are plotted against the scaled time $n_b/t^{a/b}$ for $a = b = 1$.

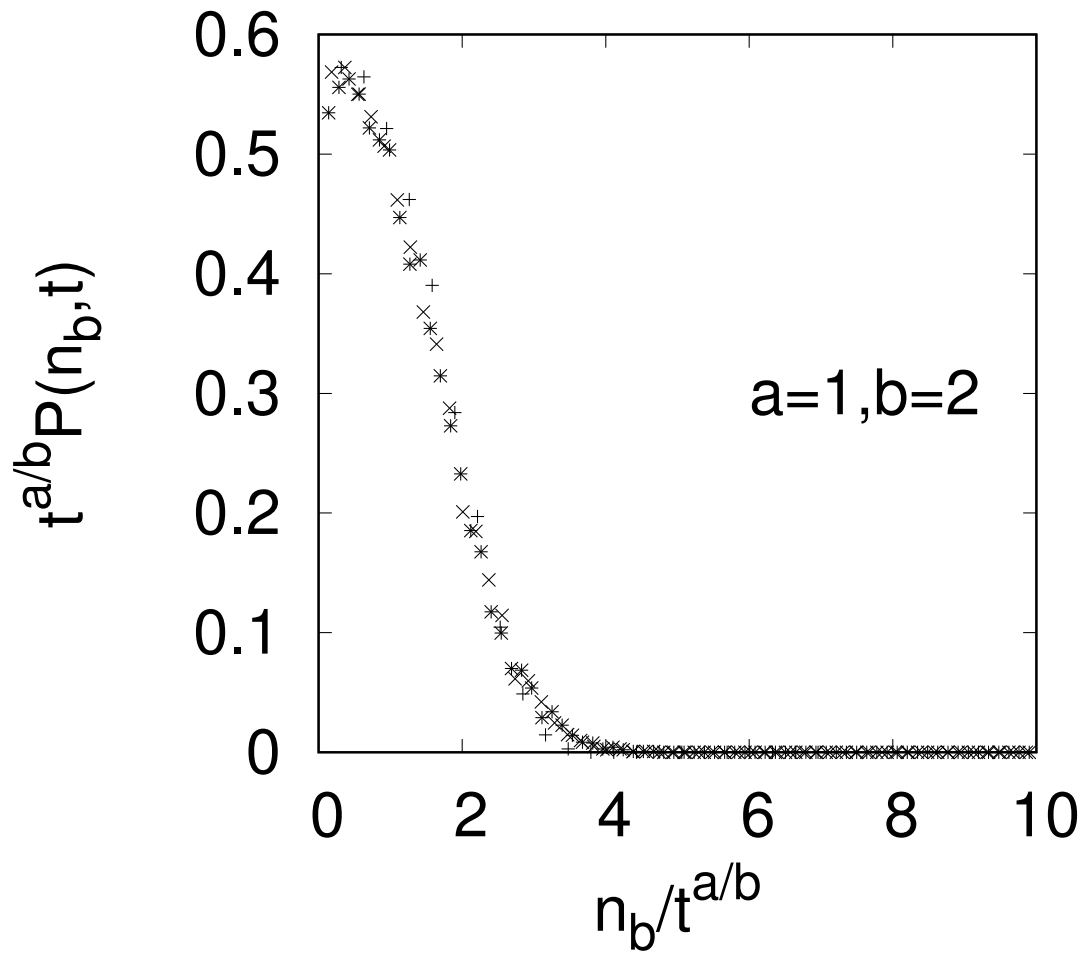


Figure 4.4: The scaled probabilities $t^{a/b}P(n_b, t)$ obtained by the same data as fig. 4.2 at $t = 10(+)$, $30(x)$, and $50(*)$ are plotted against the scaled time $n_b/t^{a/b}$ for $a = 1$ and $b = 2$.

4.4 Non-self-averaging

By using the master equation in the previous section, I will investigate non-self-averaging appearing in the balanced Polya's urn defined by eq. (4.3). Here, I will show that non-self-averaging is violated when $a = b$.

In order to study the property of self-averaging in the system, I must calculate¹ $\lim_{t \rightarrow \infty} V(n_b(t))/t^2$, where the variance is defined by $V(n_b(t)) = \langle n_b^2(t) \rangle - \langle n_b(t) \rangle^2$. The variance of Polya's urn is calculated for eq. (4.15) to investigate whether self-averaging holds or not. Using eq. (4.15), the variance of $n_b(t)$ is given by

$$\langle n_b^2(t) \rangle - \langle n_b(t) \rangle^2 = t^{2a/b} \int_0^\infty x^2 f(x) dx - t^{2a/b} \left\{ \int_0^\infty x f(x) dx \right\}^2 \quad (4.16)$$

$$\equiv t^{2a/b} A \quad (4.17)$$

where A is a constant independent of t . Eq. (4.7) shows that the total number of balls in Polya's urn is $2 + b(t - 1)$. Thus, the system size of the urn is bt in the limit of $t \rightarrow \infty$. The property of self-averaging can be analyzed by the variance divided by t^2 ,

$$V(n_b(t))/t^2 = t^{2a/b-2} A. \quad (4.18)$$

Consequently, when $a = b$, self-averaging is broken. This result agrees with the variance obtained from the exact solution of eq. (4.11) [26].

4.5 Perturbation analysis

To study the property of self-averaging of Polya's urn, I perform a perturbation analysis for this model [25]. Although the number of balls and the parameters in original Polya's urn are integers, it is natural that they may be extended to real numbers. I introduce a perturbed Polya's urn process by

$$\begin{aligned} n_a(t+1) &= n_a(t) + b\sigma_t + (b - a + \delta a(t))(1 - \sigma_t) \\ n_b(t+1) &= n_b(t) + (a + \delta a(t))(1 - \sigma_t), \end{aligned} \quad (4.19)$$

where $\delta a(t) \geq 0$, and σ_t is a random variable defined as follows: Let $\sigma_t^{n.p.}$ denote the random variable at t for a non-perturbed process. The perturbed σ_t is 1 if $\sigma_t^{n.p.} = 1$. If $\sigma_t^{n.p.} = 0$, $\sigma_t = 1$ with the probability of $\frac{n_b(t-1) - n_b^{n.p.}(t-1)}{bt}$. Otherwise, $\sigma_t = 0$. In Monte Carlo simulations, the sequence of random numbers determining σ_i is the same as that of the non-perturbed process.

¹If $\lim_{t \rightarrow \infty} V(n_b(t))/t^2 = 0$, the condition of eq. (2.5) is satisfied automatically. This statement is easily proved by using Chebyshev's theorem.

As with non-perturbed Polya's urn, a continuum approximation is applied to the above equation. The master equation of perturbed Polya's urn is given by

$$\frac{\partial P(n_b, t)}{\partial t} = -\frac{a + \delta a(t)}{bt} \frac{\partial}{\partial n_b} (n_b P(n_b, t)). \quad (4.20)$$

A general solution of this equation is

$$P(n_b, t) = \frac{g\left(n_b / \left\{t^{\frac{a}{b}} \exp\left(\int_1^t \frac{\delta a(\tau)}{b\tau} d\tau\right)\right\}\right)}{t^{\frac{a}{b}} \exp\left(\int_1^t \frac{\delta a(\tau)}{b\tau} d\tau\right)} \quad (4.21)$$

$$= \frac{g(n_b/t^{\frac{a}{b}})}{t^{\frac{a}{b}}} - \frac{n_b g'(n_b/t^{\frac{a}{b}})}{bt^{\frac{2a}{b}}} \int \frac{\delta a(\tau)}{\tau} d\tau - \frac{g(n_b/t^{\frac{a}{b}})}{bt^{\frac{a}{b}}} \int \frac{\delta a(\tau)}{\tau} d\tau \quad (4.22)$$

where I neglected terms which are higher than δa , and $g'(x_0)$ represents $dg/dx|_{x=x_0}$. Here, if $\delta a = 0$, eq. (4.22) must be equal to eq. (4.15). Therefore, I obtain $g(x) = f(x)$. Hence, the general solution is rewritten as

$$P(n_b, t) = \frac{f(n_b/t^{\frac{a}{b}})}{t^{\frac{a}{b}}} - \frac{n_b f'(n_b/t^{\frac{a}{b}})}{bt^{\frac{2a}{b}}} \int \frac{\delta a(\tau)}{\tau} d\tau - \frac{f(n_b/t^{\frac{a}{b}})}{bt^{\frac{a}{b}}} \int \frac{\delta a(\tau)}{\tau} d\tau. \quad (4.23)$$

Consider a time-discrete Polya's process that has the above asymptotic solution. One can define its response function, relaxation function and complex admittance, and investigate how the perturbation effect appears.

4.5.1 Response function

For perturbation:

$$\delta a(t) = \begin{cases} \delta a > 0 & (t = \tau), \\ 0 & (\text{otherwise}), \end{cases} \quad (4.24)$$

the response function $\phi(t, t - \tau)$ is defined by the difference $\delta n_b(t)$ between $n_b(t)$ and $n_b^{n.p.}(t)$

$$\delta n_b(t) = \sum_{\tau=1}^t \phi(t, t - \tau) \delta a(\tau) \quad (4.25)$$

where $n_b^{n.p.}(t)$ is a non-perturbed process. The response function depends on two variables t and τ because there is no time translational symmetry in Polya's urn model. Using the continuum approximation, the ensemble average of $\phi(t, t - \tau)$ is easily obtained as

$$\langle \phi(t, t - \tau) \rangle = B \frac{t^{\frac{a}{b}}}{b\tau} \quad (4.26)$$

where

$$B = \int_0^\infty x f(x) dx. \quad (4.27)$$

Derivation

By the definition of the response function, one obtains

$$\langle \phi(t, t - \tau) \rangle = \frac{\langle n_b(t) \rangle - \langle n_b^{n.p.}(t) \rangle}{\delta a} \quad (4.28)$$

for $\delta a(t) = \delta a \delta(t - \tau)$. From eq. (4.23), $\langle n_b(t) \rangle$ is given by

$$\begin{aligned} \langle n_b(t) \rangle &= \langle n_b^{n.p.}(t) \rangle - t^{\frac{a}{b}} \int \frac{df}{dx} \frac{x^2}{b} dx \int \frac{\delta a \delta(t' - \tau)}{t'} dt' \\ &\quad - t^{\frac{a}{b}} \int f(x) \frac{x}{b} dx \int \frac{\delta a \delta(t' - \tau)}{t'} dt' \\ &= \langle n_b^{n.p.}(t) \rangle + t^{\frac{a}{b}} \int x f(x) dx \frac{\delta a}{b\tau}. \end{aligned} \quad (4.29)$$

Thus, eq. (4.26) holds.

Time dependence of the average of response function is given by $t^{a/b}$. Since I define non-self-averaging by the variance divided by the size, the reduced response function is defined by $\phi(t, t - \tau)/t$. Now, the system size is given by $\sim O(t)$. The average of the reduced response function $\langle \phi(t, t - \tau) \rangle/t$ decreases with increasing time when $a < b$. For $a = b$, the average of the reduced function does not decay to 0.

Figures 4.5 and 4.6 show a few samples of reduced response functions $\phi(t, t - 10)/t$ and the averages of all samples for $a = b = 1$ and $a = 1, b = 2$. The number of samples is 10^5 . The reduced response function of each sample has discontinuous increasing points. For $a = 1$ and $b = 2$, the average of $\phi(t, t - 10)/t$ decays to 0 as $t \rightarrow \infty$. In contrast, in $a = b$, the average of $\phi(t, t - 10)/t$ does not decay to 0. Discontinuous increases play an important role in the absence of decay in the average of the reduced response function. For some samples, $\phi(t, t - 10)/t$ sometimes increases discontinuously. If such increases do not occur, the average of the reduced response function will eventually vanish. However, the frequency of discontinuous increases is larger than the decay rate of the reduced response function, and $\langle \phi(t, t - \tau) \rangle/t$ does not decay to 0.

4.5.2 Relaxation function

Here, I consider the process with the following step-function type perturbation:

$$\delta a(t) = \begin{cases} \delta a & (1 < t < \tau) \\ 0 & (\tau < t). \end{cases} \quad (4.30)$$

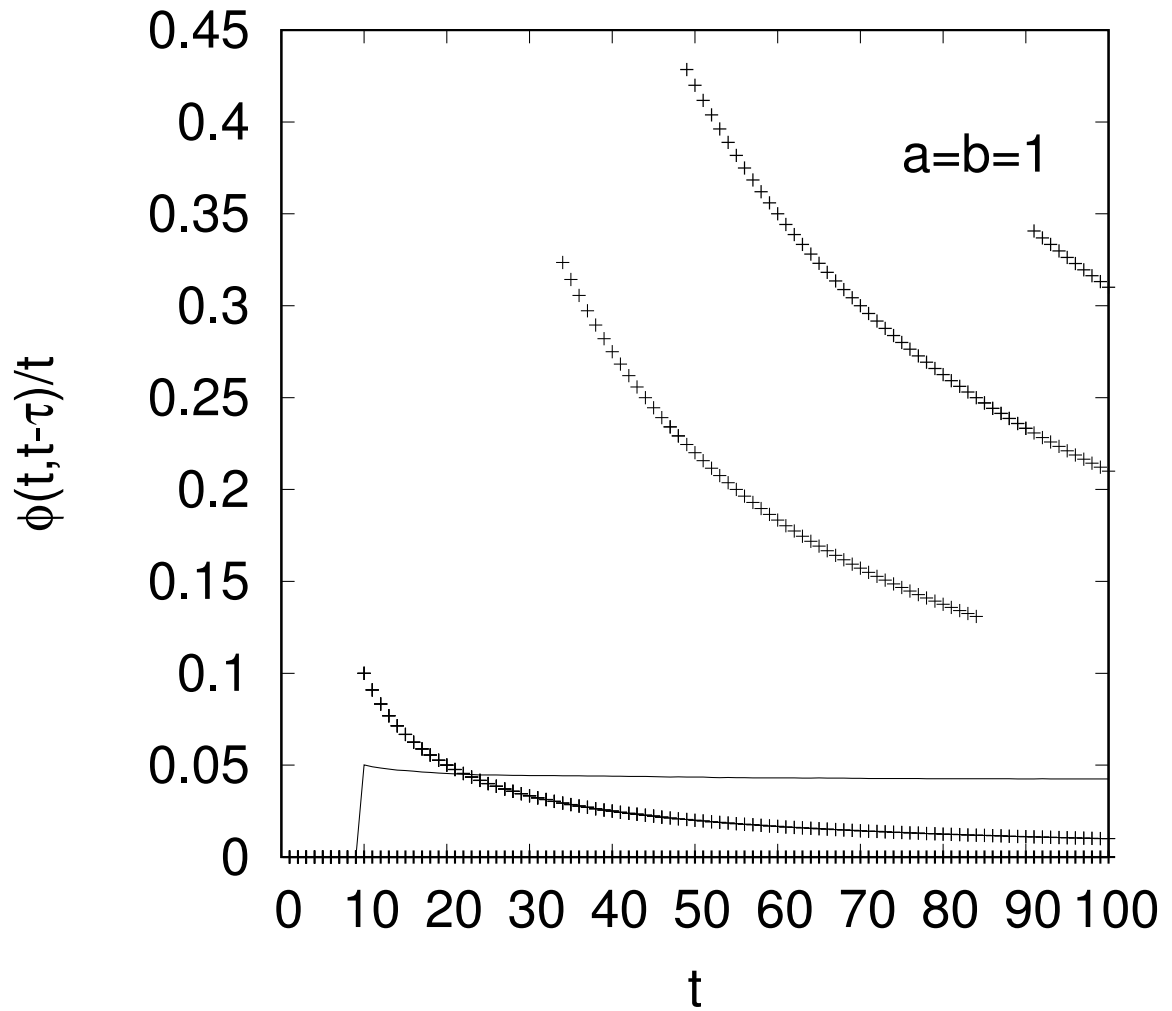


Figure 4.5: The response function $\phi(t, \tau)$ divided by time t (the reduced response function) for $a = b = 1$ at $\tau = 10$. The solid curve is the average over 10^5 samples. Various symbols represent the time series for five typical samples.

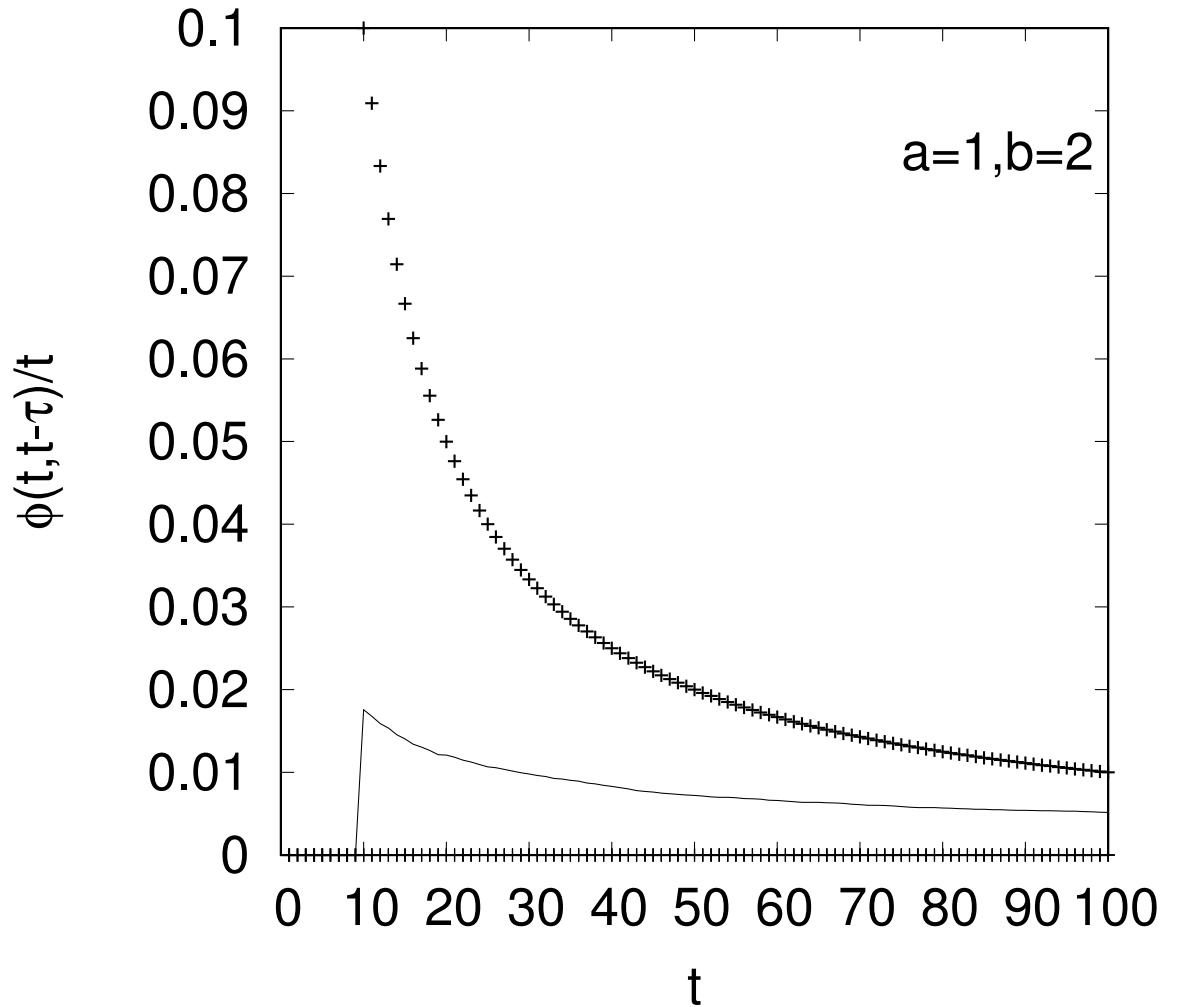


Figure 4.6: The response function $\phi(t, \tau)$ divided by time t (the reduced response function) for $a = 1$, and $b = 2$ at $\tau = 10$. The solid curve is the average over 10^5 samples. Various symbols represent the time series for five typical samples.

For this perturbation, the relaxation function is defined by

$$\delta n_b(t) = \psi(t, t - \tau) \delta a. \quad (4.31)$$

From eq. (4.22), the average of the relaxation function is

$$\langle \psi(t, t - \tau) \rangle = \begin{cases} \frac{B}{b} t^{\frac{a}{b}} \ln t & (t < \tau) \\ \frac{B}{b} t^{\frac{a}{b}} \ln \tau & (t > \tau). \end{cases} \quad (4.32)$$

Derivation

Here, I only consider the case^a $t < \tau$. By the definition of the function,

$$\langle \psi(t, t - \tau) \rangle = \frac{\langle n_b(t) \rangle - \langle n_b^{n.p.}(t) \rangle}{\delta a} \quad (4.33)$$

for the perturbation defined as eq. (4.30). From eq. (4.23), $\langle n_b(t) \rangle$ is given by

$$\begin{aligned} \langle n_b(t) \rangle &= \langle n_b^{n.p.}(t) \rangle - t^{\frac{a}{b}} \int \frac{df}{dx} \frac{x^2}{b} dx \int_1^t \frac{\delta a}{t'} dt' \\ &\quad - t^{\frac{a}{b}} \int f(x) \frac{x}{b} dx \int_1^t \frac{\delta a}{t'} dt' \\ &= \langle n_b^{n.p.}(t) \rangle + t^{\frac{a}{b}} \int x f(x) dx \frac{\delta a}{b} \ln t. \end{aligned} \quad (4.34)$$

Thus, eq. (4.32) is obtained.

^aThis derivation holds also for $t > \tau$.

For later convenience, a reduced relaxation function is defined by $\psi(t, t - \tau)/t$.

Figures 4.7 and 4.8 show reduced relaxation functions $\psi(t, t - \tau)/t$ for $a = b = 1$ and $a = 1, b = 2$. The relaxation function is similar to the reduced response function in that they do not decay to zero for $a = b = 1$ and decay to zero for $a = 1, b = 2$.

Figure 4.8 shows a discontinuous increase even for $a = 1$ and $b = 2$. The probability of the discontinuous increase is larger in the relaxation function than that in the response function within $t \leq 10$. This is because the perturbation in the relaxation function is given by the step function.

4.5.3 Complex admittance

The complex admittance $\chi(t, \omega)$ is defined by

$$\delta n_b(t) = \chi(t, \omega) \delta a \exp(-i\omega t) \quad (4.35)$$

where the perturbation $\delta a(t)$ is

$$\delta a(t) = \delta a \exp(-i\omega t). \quad (4.36)$$

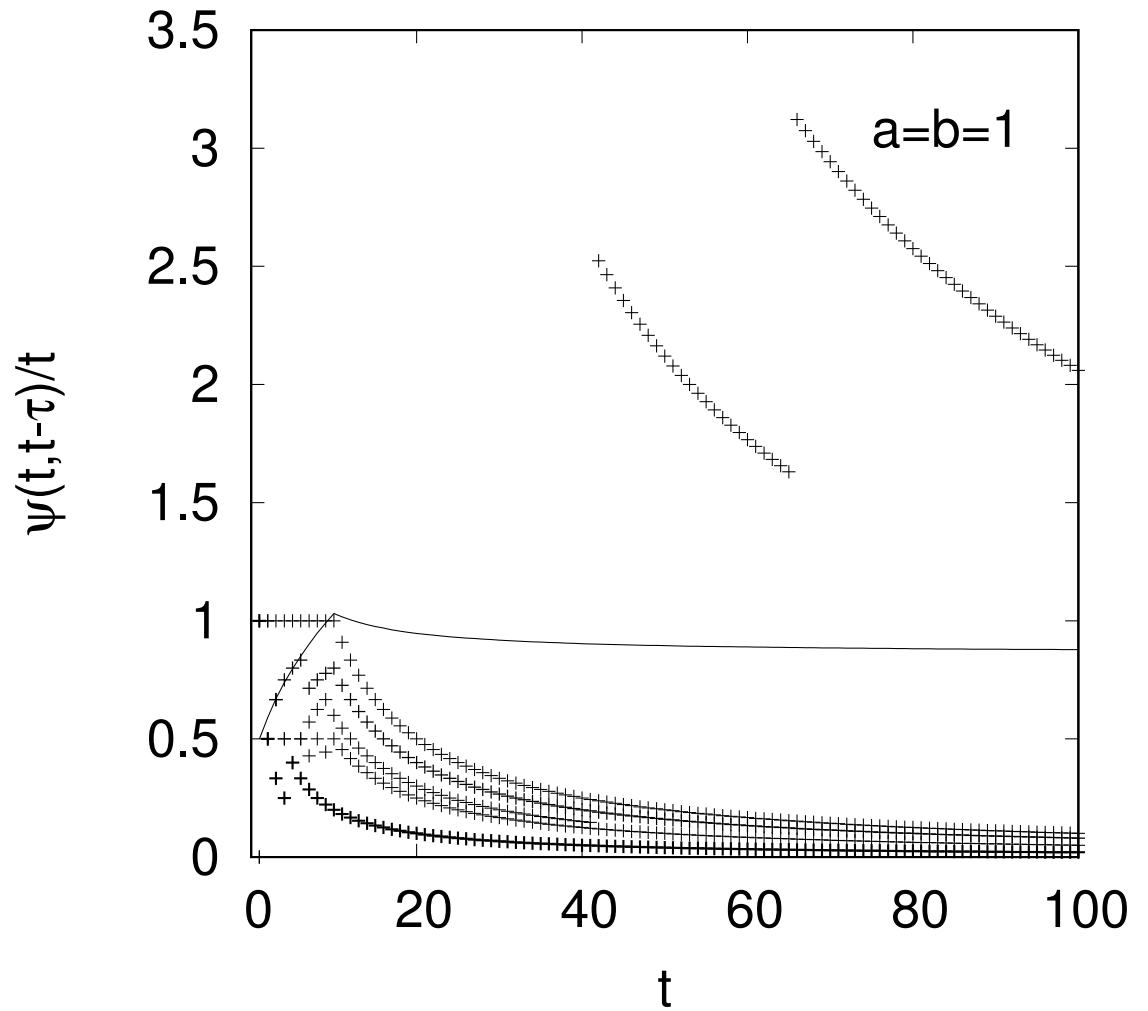


Figure 4.7: The relaxation function $\psi(t, t-\tau)$ divided by time t for $a = b = 1$ where $\tau = 10$. The solid curve is the average over 10^5 samples. Various symbols represent the time series for five typical samples.

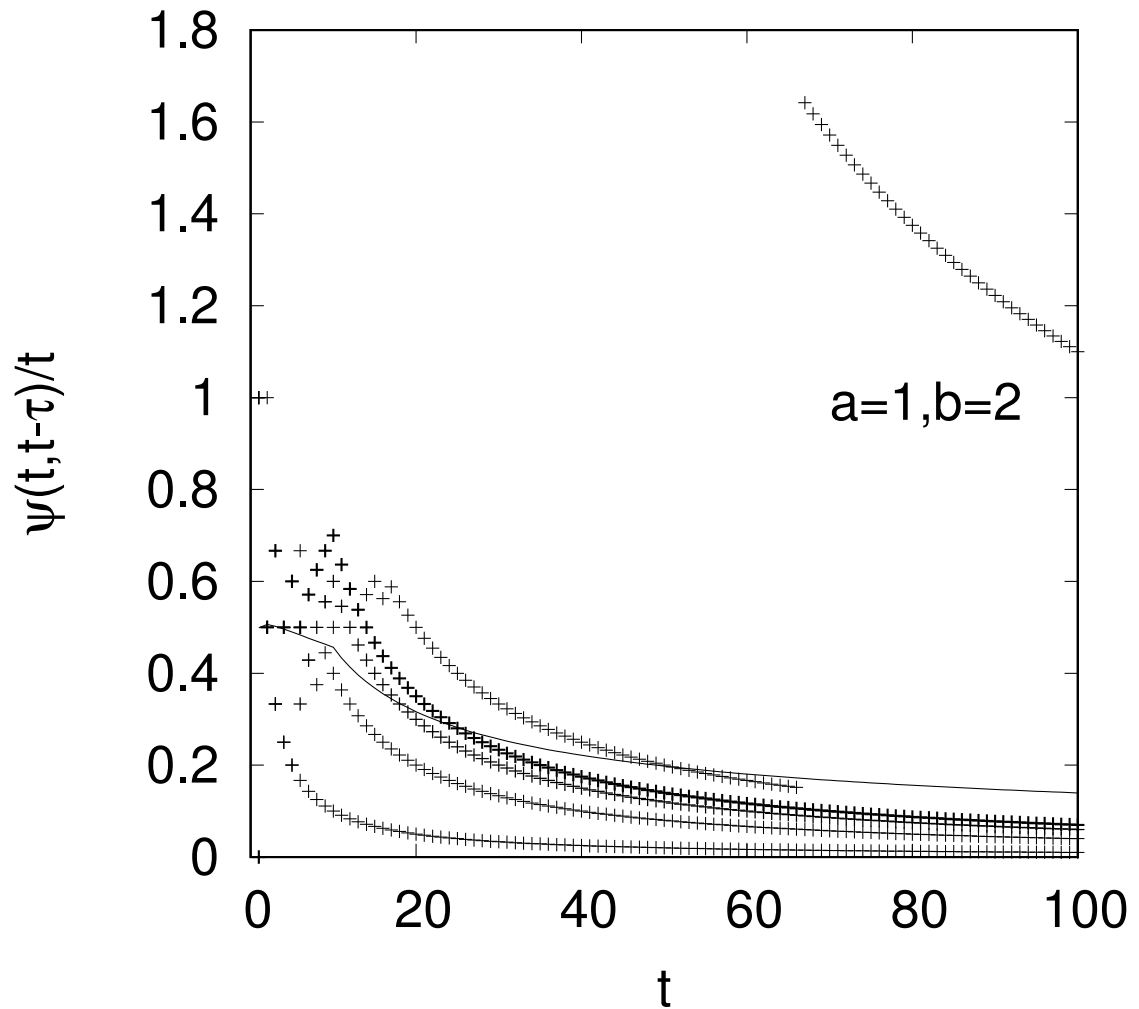


Figure 4.8: The relaxation function $\psi(t, t - \tau)$ divided by time t for $a = 1$, $b = 2$, where $\tau = 10$. The solid curve is the average over 10^5 samples. Various symbols represent the time series for five typical samples.

With the continuum approximation, an analytic form of the average of the complex admittance is obtained:

$$\langle \chi(t, \omega) \rangle = \frac{t^{\frac{a}{b}} B}{b} \int_1^t \frac{\exp(i\omega(t - \tau))}{\tau} d\tau. \quad (4.37)$$

Derivation

By the definition of the function,

$$\langle \chi(t, t - \tau) \rangle = \frac{[\langle n_b(t) \rangle - \langle n_b^{n.p.}(t) \rangle] \exp(i\omega t)}{\delta a} \quad (4.38)$$

for the perturbation defined as $\delta a \exp(-i\omega t)$. From eq. (4.23), $\langle n_b(t) \rangle$ is given by

$$\begin{aligned} \langle n_b(t) \rangle &= \langle n_b^{n.p.}(t) \rangle - t^{\frac{a}{b}} \int \frac{df}{dx} \frac{x^2}{b} dx \int \frac{\delta a \exp(-i\omega\tau)}{\tau} d\tau \\ &\quad - t^{\frac{a}{b}} \int f(x) \frac{x}{b} dx \int \frac{\delta a \exp(-i\omega\tau)}{\tau} d\tau \\ &= \langle n_b^{n.p.}(t) \rangle + t^{\frac{a}{b}} \int x f(x) dx \int \frac{\delta a \exp(-i\omega\tau)}{\tau} d\tau \end{aligned} \quad (4.39)$$

Thus, eq. (4.32) is obtained.

In the calculation of $\chi(t, \omega)$, instead of calculating the Fourier transformation of $\delta n_b(t)$, I use the following identity

$$\begin{aligned} \chi(t, \omega) &= \chi_R(t, \omega) + \chi_I(t, \omega) \\ &= \frac{\delta n_b^{cos}}{\delta a} \cos(\omega t) + \frac{\delta n_b^{sin}}{\delta a} \sin(\omega t) \\ &\quad + i \left\{ \frac{\delta n_b^{sin}}{\delta a} \cos(\omega t) - \frac{\delta n_b^{cos}}{\delta a} \sin(\omega t) \right\} \end{aligned} \quad (4.40)$$

where δn_b^{cos} (δn_b^{sin}) is calculated by applying perturbation $\delta a \cos(\omega t)$ ($\delta a \sin(\omega t)$). The reduced complex admittance is defined by $\chi(t, \omega)/t$.

In figs. 4.9, and 4.10 the absolute values of the average of the reduced complex admittance $\langle \chi(t, \omega) \rangle/t$ are plotted against ω at $t = 10, 50$, and 100 . The absolute values of $\chi(t, \omega)/t$ have the peak at about 6.4 . When $a = b = 1$, the amplitude of the reduced admittance does not change with time. However, when $a = 1$ and $b = 2$, the amplitude seems to decay to 0 as seen in fig. 4.11.

4.6 Conclusions

In the former of this chapter, the behavior of $n_b(t)$ was studied by using the continuum approximation and Monte Carlo simulations. The calculation results show that

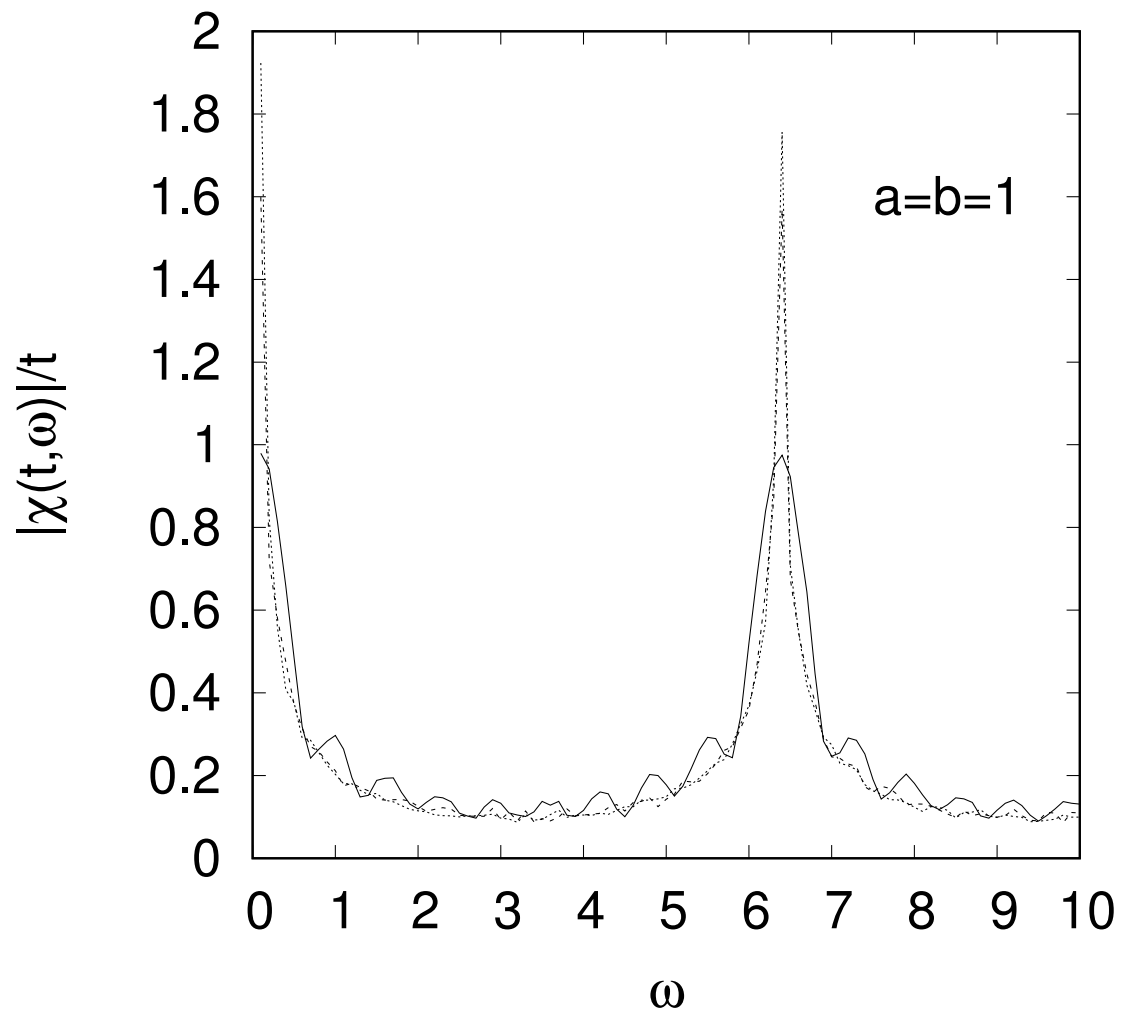


Figure 4.9: The absolute value of $\langle \chi(t, \omega) \rangle$ divided by time t at $t = 10$ (solid line), 50 (dashed line), and 100 (dotted line) for $a = b = 1$.

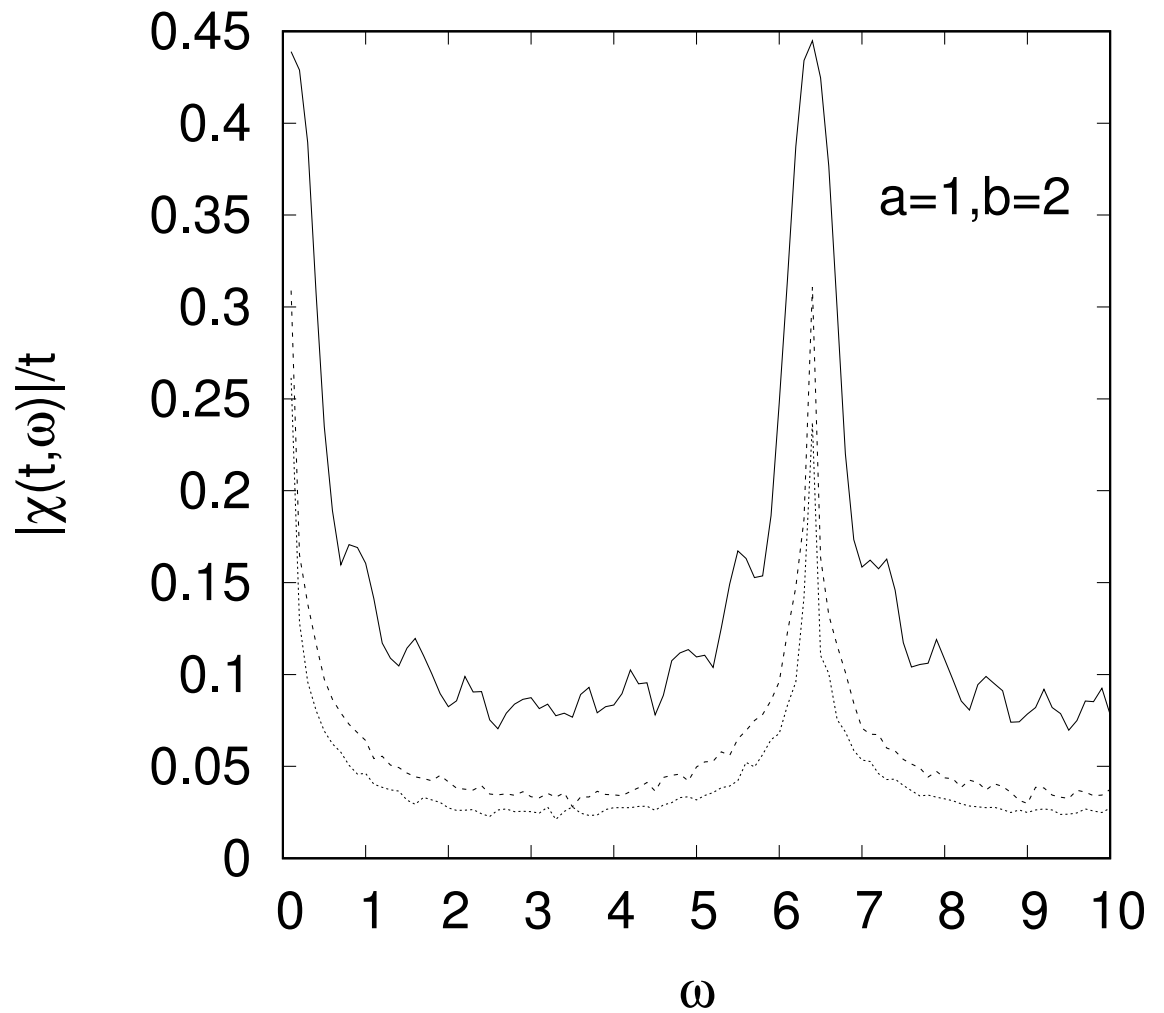


Figure 4.10: The absolute value of $\langle \chi(t, \omega) \rangle$ divided by time t at $t = 10$ (solid line), 50 (dashed line), and 100 (dotted line) for $a = 1$, $b = 2$.

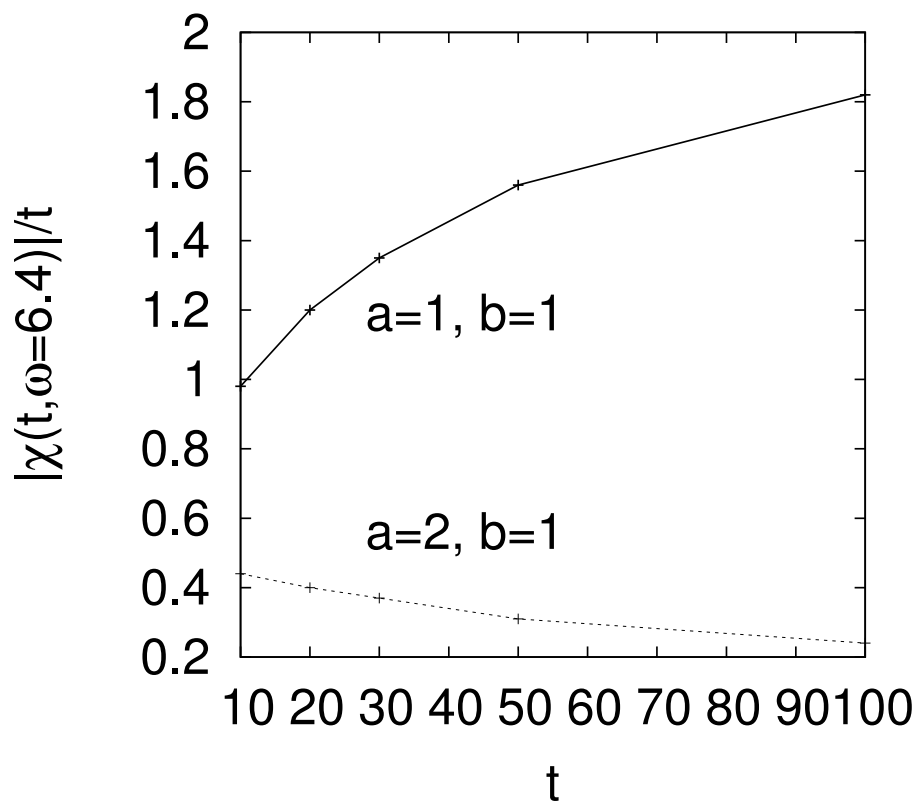


Figure 4.11: The time dependence of the absolute value $\langle \chi(t, \omega) \rangle$ divided by time t at $\omega = 6.4$ for $a = b = 1$ (solid line) and $a = 1, b = 2$ (dotted line)

the variance of $n_b(t)/t \propto t^{2a/b-2}$ does not decay to 0 only if $a = b$. Consequently, by the discussion below the definition of self-averaging (section 2.1), one can find that $n_b(t)$ is non-self-averaging when $a = b$.

In the latter of this chapter, new perturbed Polya's urn processes were proposed to investigate the effects of non-self-averaging on the time evolution of $n_b(t)$. These properties were analyzed by considering the response function, the relaxation function and the complex admittance. These analyses demonstrated the relation between non-self-averaging properties in the Polya's urn and the response function or the relaxation function. If self-averaging is violated, then the averages of the reduced response function, the relaxation function, and the absolute values of complex admittance do not decay to 0. When self-averaging holds, these functions converge to 0. Some samples of the response functions and the relaxation functions increase discontinuously. The averages of these functions do not decay to 0 because of the discontinuous increases when these self-averaging is violated.

Chapter 5

Non-linear Polya's urn model

5.1 Introduction

In the previous chapter, I showed the relation between non-self-averaging and the linear response for balanced Polya's urn processes. Balanced Polya's urn is featured by the matrix of the urn

$$\alpha = b \tag{5.1}$$

$$\beta = 0 \tag{5.2}$$

$$\gamma = b - a \tag{5.3}$$

$$\delta = a, \tag{5.4}$$

where these parameters represent increments in the number of balls. The numbers of white balls and black balls at time t are denoted by $n_a(t)$ and $n_b(t)$, respectively, and $n_a(t+1)$ and $n_b(t+1)$ are given by eq. (4.1). It became clear that self-averaging is violated when $a = b$. Non-self-averaging was related to the linear response functions, such as the average of reduced response function, the reduced relaxation function and the reduced complex admittance. Namely, if self-averaging is violated, the average of the reduced functions do not decay to 0.

Does this relation hold universally? To answer this question, I consider more general Polya's urn models. One can generalize the rule of drawing balls by introducing a non-linear function $Q(x)$ for the probability of drawing the black ball. For Polya's urn in the previous chapter, the probability of drawing black balls is simply the fraction of the black balls x_b . For non-linear Polya's urn, the above probability is replaced by a non-linear probability $Q(x_b)$ which satisfies $0 \leq Q(x) \leq 1$ in $0 \leq x \leq 1$.

Originally, Arthur *et al.* [27] proposed this model to study the market in which two competitive products A and B exist. In this case, each person chooses only

one product out of the two. For example, let us imagine the share of smart phones. People buy mostly iPhone or Android, but usually do not get both of them. For simplicity, Arthur *et al.* assumed that consumers do not have any information on products A and B . However, at time t , the consumers know the numbers of the products A (B) that have been sold up to time t , which will be described by $n_a(t)$ ($n_b(t)$). Arthur *et al.* assumed that they choose the product B with the probability $Q(x_b)$, where $x_b \stackrel{\text{def}}{=} n_b(t)/(n_a(t)+n_b(t)$; $Q(x_b)$ is the weighting function. This assumption is natural, and one can imagine popular movies or songs. One of the reasons for their popularity is that they are favored by many people. These processes of decision-making were described by non-linear Polya's urn using the correspondence of $n_a(t)$ and $n_b(t)$ with the number of white and black balls.

In this chapter, non-linear Polya's urn model is investigated by the continuum approximation and a perturbation analysis. I show the asymptotic behaviors in the long time limit. The condition of self-averaging for non-linear Polya's urn is different from that for linear Polya's urn. I study how this difference affects the relation between non-self-averaging and linear response.

First, I formulate the master equation in the model using the continuum approximation. Second, I show that self-averaging is violated when the number of the stable fixed points of the urn is larger than 1. Here, fixed points of the urn correspond to the positions of peaks of the distribution $P(x_b, t)$ in the long time limit. Third, I apply a delta-function-like perturbation to non-linear Polya's urn and study the response function. Finally, I summarize this chapter as follows: (1) the equilibrium distribution of x_b has several peaks. (2) Non-self-averaging is not always related to the behavior of the reduced response function $\phi(t, t - \tau)/t$.

5.2 Definition of non-linear Polya's urn and the master equation

Non-linear Polya's urn model is defined as follows: In Section 4.1, I have introduced a random variable σ_t . The probability distribution of random variable now reads

$$\text{Prob}(\sigma_t = 0) = 1 - Q(x_b),$$

and

$$\text{Prob}(\sigma_t = 1) = Q(x_b),$$

where $\text{Prob}(\text{event})$ means the probability that the event occurs, and $x_b = n_b/N(t) \simeq n_b/bt$. Therefore, the master equation is given by

$$P(n_b, t + 1) = Q \left(\frac{n_b - a}{N(t)} \right) P(n_b - a, t) + \left(1 - Q \left(\frac{n_b}{N(t)} \right) \right) P(n_b, t), \quad (5.5)$$

where $P(n_b, t)$ represents the distribution of n_b at t . The initial condition is given by $P(n_b, 1) = \delta_{1, n_b}$. A boundary condition for this equation is $P(0, t) = 0$ when $t > 1$. From eq. (5.5), I can find $P(n_b, t) = 0$ for $n_b > 1 + b(t - 1)$.

When $n_b \gg a$, and $t \gg 1$, the discrete master equation can be approximated as

$$\frac{\partial P(n_b, t)}{\partial t} = -a \frac{\partial}{\partial n_b} \left[Q \left(\frac{n_b}{bt} \right) P(n_b, t) \right]. \quad (5.6)$$

5.3 Non-self-averaging

To study the property of self-averaging, I calculate the variance of n_b/t in the long time limit. Since $x_b = n_b/bt$, I consider the distribution of x_b at t denoted by $G(x_b, t)$ instead of $P(n_b, t)$. The behavior of the distribution in the long time limit was studied by Arthur *et al* [27]. Here, I show the behavior using a different method.

First, I show that the distribution function $G(x_b, t)$ obeys

$$\frac{\partial G(x_b, t)}{\partial t} = -\frac{1}{bt} \frac{\partial}{\partial x_b} [aQ(x_b)G(x_b, t) - bx_bG(x_b, t)], \quad (5.7)$$

where I restrict the range of x_b to $0 \leq x_b \leq 1$, and require the boundary conditions that the flux of the distribution, $(aQ(x_b) - bx_b)G(x_b, t)$, vanishes at $x_b = 1$ and $x_b = 0$ because the probability distribution $G(x_b, t)$ is conserved.

Proof of eq. (5.7):

The relation between $G(x_b, t)$ and $P(n_b, t)$ is

$$G(x_b, t) = P(n_b, t) \frac{dn_b}{dx_b} = btP(bt x_b, t). \quad (5.8)$$

Substitution of $P(n_b, t) = G(n_b/t, t)/bt$ into eq. (5.6) leads to

$$\frac{\partial}{\partial t} \frac{G(n_b/bt, t)}{bt} = -\frac{a}{b^2 t^2} \frac{\partial}{\partial x_b} Q(x_b) G(n_b/bt, t). \quad (5.9)$$

The derivative on the left-hand side reads

$$-\frac{1}{bt^2} G(x_b, t) - \frac{x_b}{t} \frac{\partial G(x_b, t)}{\partial x_b} + \frac{1}{bt} \frac{\partial G(x_b, t)}{\partial t}. \quad (5.10)$$

Therefore, eq. (5.7) is obtained. *Q. E. D*

The fixed points of the urn are defined as the solutions of

$$aQ(x_b) - bx_b = 0, \quad (5.11)$$

which will be denoted by $\{x_i | i = 1, \dots, l\}$ with l being the number of the fixed points. Eq. (5.7) can be rewritten as

$$\frac{\partial G(x_b, t)}{\partial t} = -\frac{1}{bt} \frac{\partial}{\partial x_b} [f(x_b)G(x_b, t)], \quad (5.12)$$

where $f(x_b) \stackrel{\text{def}}{=} aQ(x_b) - bx_b$. Now, I derive the asymptotic distribution $G_e(x_b) \stackrel{\text{def}}{=} \lim_{t \rightarrow \infty} G(x_b, t)$ from the master equation (5.12). One can define the following Lyapunov functional $V[G]$:

$$V[G] = \int_0^1 dx_b G(x_b, t) \int_0^{x_b} dx' f(x'). \quad (5.13)$$

Since

$$\begin{aligned} \int_0^{x_b} dx' f(x') &= \int_0^{x_b} dx_b \{aQ(x_b) - bx_b\} \\ &\leq ax_b - \frac{bx_b^2}{2} \\ &\leq \frac{a^2}{2b} \end{aligned} \quad (5.14)$$

because $Q(x_b) \leq 1$, I have

$$V[G] \leq \int_0^1 dx_b G(x_b, t) \frac{a^2}{2b}. \quad (5.15)$$

Obviously, $\int_0^1 dx_b G(x_b, t)$ is equal to 1 because of the normalization. Therefore, $V[G]$ has an upper bound $a^2/2b^2$. The time variation of $V[G]$ is given by

$$\begin{aligned} \frac{dV[G]}{dt} &= \int_0^1 dx_b \frac{\partial G(x_b, t)}{\partial t} \int_0^{x_b} dx' f(x') \\ &= -\frac{1}{bt} \int_0^1 dx_b \frac{\partial f(x_b)G(x_b, t)}{\partial x_b} \int_0^{x_b} dx' f(x') \\ &= -\left[\frac{1}{bt} f(x_b)G(x_b, t) \int_0^{x_b} dx' f(x') \right]_0^1 + \frac{1}{bt} \int_0^1 dx_b \{f(x_b)\}^2 G(x_b, t) \\ &= \frac{1}{bt} \int_0^1 dx_b \{f(x_b)\}^2 G(x_b, t). \end{aligned} \quad (5.16)$$

The right-hand side of eq. (5.16) is non-negative. Thus, for any initial function $G(x_b, 0)$, the Lyapunov functional $V[G]$ increases monotonically with time. Since

$V[G]$ has an upper bound, the existence of $G_e(x_b)$ is guaranteed¹, and

$$\left. \frac{dV[G]}{dt} \right|_{G(x_b,t)=G_e(x_b)} = 0. \quad (5.17)$$

Hence, one can obtain

$$\{f(x_b)\}^2 G_e(x_b) = 0. \quad (5.18)$$

Therefore, if $f(x_b) \neq 0$, $G_e(x_b) = 0$.

Although eq. (5.18) leads to $G_e(x_b)$ except at x_i 's satisfying $f(x_i) = 0$, the value of $G_e(x_b)$ cannot be determined at x_i 's, because the value of $G_e(x_i)$ depends on the stability of x_i . To obtain the value of $G_e(x_i)$, I expand $G(x_b, t)$ and $f(x_b)$ in eq. (5.7) at x_i . For the first order of $x_b = x_i + \delta x$, I obtain the equation

$$\frac{dG(x_i, t)}{dt} + \frac{dG'(x_i, t)}{dt} \delta x = -\frac{1}{bt} \left(\frac{\partial}{\partial \delta x} [f' \delta x (G(x_i, t) + G'(x_i, t) \delta x)] \right), \quad (5.19)$$

where $G'(x_i, t) = \partial G(x_b, t) / \partial x_b|_{x_b=x_i}$, and $f'(x_i) \stackrel{\text{def}}{=} df(x_b) / dx_b|_{x_b=x_i}$. To obtain eq. (5.19), I used $f(x_i) = 0$. The zeroth order contribution of the above equation reads

$$\frac{dG(x_i, t)}{dt} = -\frac{f'(x_i)}{bt} G(x_i, t). \quad (5.20)$$

By integrating eq. (5.20), one can get

$$G(x_i, t) = \gamma(x_i) t^{-f'(x_i)/b}, \quad (5.21)$$

where $\gamma(x_i)$ is a constant of integration. From eq. (5.21), one finds that

$$G_e(x_i) \rightarrow \infty. \quad (5.22)$$

if x_i is a stable fixed point, i.e., $x_i \in \{x_i | f(x_i) = 0 \text{ and } f'(x_i) < 0\}$.

Consequently, if the stable fixed points are isolated, I have

$$G_e(x_b) = \sum_i \rho_i \delta(x_b - x_i^{st}), \quad (5.23)$$

where ρ_i is a coefficient satisfying the condition $\sum_i \rho_i = 1$, and x_i^{st} is the stable fixed point.

When the number of stable fixed points is larger than one, the variance of $n_b/t (= bx_b/t)$ does not decay to 0 in the long time limit:

$$\begin{aligned} V(n_b/t) &= b^2 V(x_b) \\ &= b^2 \left\{ \sum_{i=1}^k \rho_i (x_i^{st})^2 - \left(\sum_{i=1}^k \rho_i x_i^{st} \right)^2 \right\}, \end{aligned} \quad (5.24)$$

¹Even if $G \neq G_e$, $dV/dt \rightarrow 0$ in the long time limit because of the factor $1/bt$ in the right hand side of eq. (5.16). However, at finite time, dV/dt is always larger than 0. Thus, the distribution G approaches G_e at every time.

where k represents the number of the stable fixed points. If $k = 1$, $V(n_b/t) = 0$ because $\rho_1 = 1$. Equation (5.24) is not zero in the long time limit when $k \geq 2$ and the number of non-zero ρ_i 's is larger than 1. Note that non-self-averaging is determined by the number of stable fixed points for any values of a and b .

In the case of linear Polya's urn, $Q(x_b) = x_b$. When $a = b$, this process is non-self-averaging. In the case of $a \neq b$, self-averaging holds. If $Q(x_b) = x_b$,

$$f(x_b) = (a - b)x_b. \quad (5.25)$$

Therefore, when $a \neq b$, fixed point is only $x^{st} = 0$, that is, the number of stable fixed points is one. However, for $a = b$, the number of stable fixed points is infinite because an arbitrary $x_b \in [0, 1]$ satisfies $f(x_b) = 0$.

Consequently, one can interpret the relationship between non-self-averaging and the number of stable fixed points from a unified theoretical viewpoint. (1) When the number of stable fixed point is 1, self-averaging holds. (2) If the number of stable fixed points is higher than 1, self-averaging is violated. (3) In the case that $a = b$ and $Q(x_b) = x_b$, the number of stable fixed points is infinite, and self-averaging does not hold.

5.4 Numerical example

In this section, I calculate numerically the distributions for two specific forms of $Q(x)$. Here, numerical calculations support the long-time behavior of the distribution $G(x_b, t)$ discussed in the previous section.

5.4.1 Example 1

In the first example, I choose

$$Q(x) = \begin{cases} 2^{\beta-1}(x - \frac{1}{2})^\beta + \frac{1}{2} & (x \geq 1/2) \\ -2^{\beta-1}(\frac{1}{2} - x)^\beta + \frac{1}{2} & (x < 1/2), \end{cases} \quad (5.26)$$

where β is a non-negative parameter. The master equation in the continuum approximation is

$$\frac{\partial G(x_b, t)}{\partial t} = \begin{cases} \frac{\partial}{\partial x_b} \{ (a [2^{\beta-1}(x - \frac{1}{2})^\beta + \frac{1}{2}] - bx_b) G(x_b, t) \} & (x \geq 1/2) \\ \frac{\partial}{\partial x_b} \{ (a [-2^{\beta-1}(\frac{1}{2} - x)^\beta + \frac{1}{2}] - bx_b) G(x_b, t) \} & (x < 1/2). \end{cases} \quad (5.27)$$

Figure 5.1 shows the functional form of $Q(x)$ for $\beta = 0.5$ and $\beta = 2$. If $\beta > 1$, and $a = b = 1$, a stable fixed point is at $x = 1/2$. When $\beta < 1$, and $a = b = 1$, stable fixed points are at $x = 0$ and 1. Figures 5.2 and 5.3 show the distributions $G(x_b, t)$

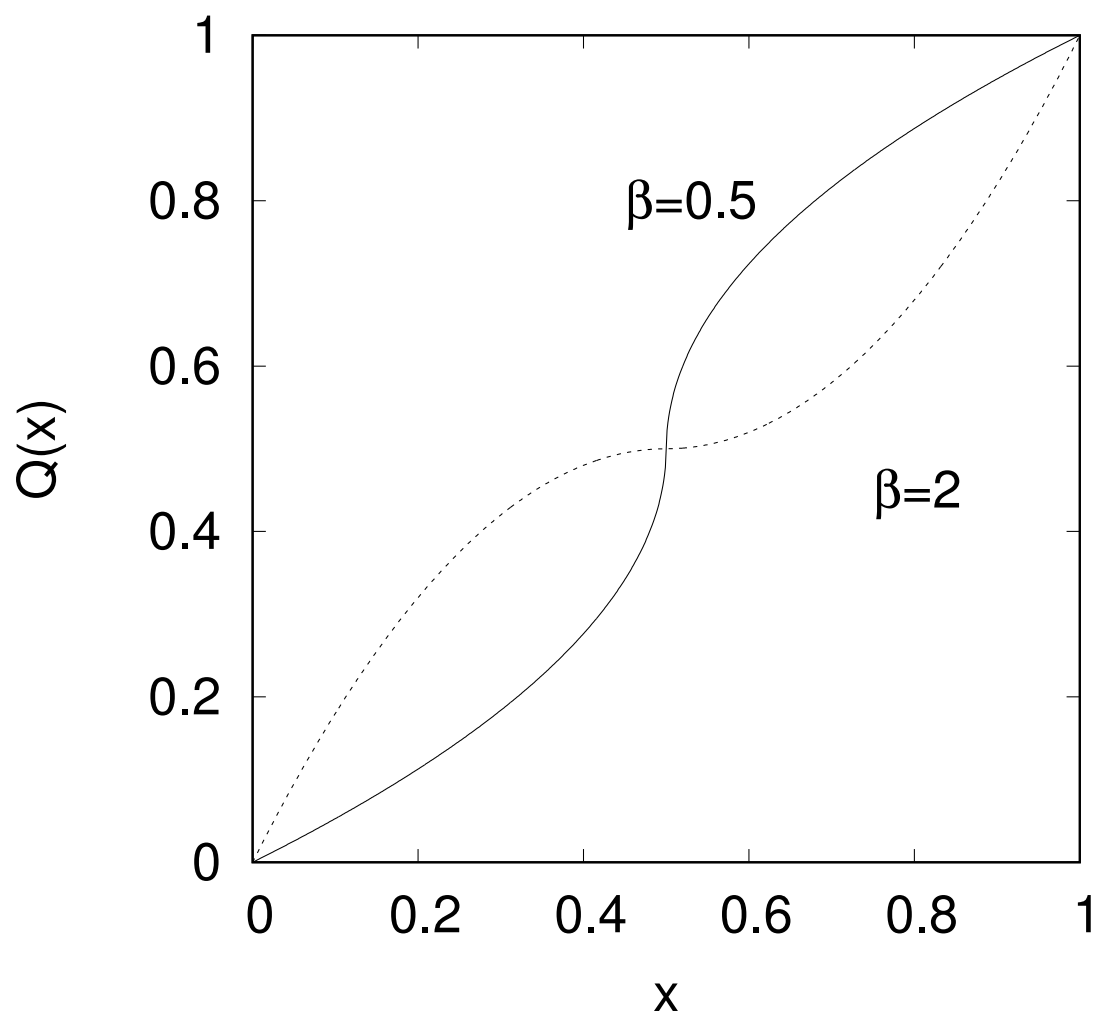


Figure 5.1: The x dependence of the probability of drawing the black ball $Q(x)$ given by eq. (5.26) for $\beta = 0.5$ and 2.

at $t = 100, 1000$, and 10000 . As time t increases, the distributions are localized around stable fixed points.

5.4.2 Example 2

Let us choose

$$Q(x) = \frac{1}{2} \tanh \left\{ \beta \left(x - \frac{1}{2} \right) \right\} + \frac{1}{2}, \quad (5.28)$$

where $\beta \geq 0$. The master equation in the continuum approximation is

$$\frac{\partial G(x_b, t)}{\partial t} = \frac{\partial}{\partial x_b} \left\{ \left(a \left[\frac{1}{2} \tanh \left\{ \beta \left(x - \frac{1}{2} \right) \right\} + \frac{1}{2} \right] - bx_b \right) G(x_b, t) \right\}. \quad (5.29)$$

Figure 5.4 shows the functional form of $Q(x)$ for $\beta = 0.1$ and $\beta = 5$.

The form of $G_e(x_b)$ depends on the value of β . When $\beta > 2a/b$, the number of the stable fixed points is two. Therefore, the stationary distribution is

$$G_e(x_b) = \rho \delta(x_b - x_l^{st}) + (1 - \rho) \delta(x_b - x_h^{st}), \quad (5.30)$$

where ρ is a coefficient determined by the initial condition of $G(x_b, t)$, and x_l^{st} and x_h^{st} are stable fixed points. In the case of $\beta < 2a/b$, the number of the stable fixed point is one. The stationary distribution is

$$G_e(x_b) = \delta(x_b - x_o^{st}), \quad (5.31)$$

where x_o^{st} is a stable fixed point. If $\beta = 2a/b$, stable fixed points do not exist.

Figure 5.5 shows the behavior of $G(x_b, t)$ at time $t = 50000$ for various β . When $\beta = 0.1$, and $\beta = 5.0$, fig. 5.5 agrees with the distributions given by eqs. (5.30) and (5.31). When $\beta = 2$, the distribution $G(x_b, t)$ in fig. 5.5 is broad around a neutral fixed point $1/2$.

5.5 Perturbation analysis

If a perturbation is denoted by $\delta a(t)$, the master equation (5.6) becomes

$$\frac{\partial P(n_b, t)}{\partial t} = -(a + \delta a(t)) \frac{\partial}{\partial n_b} Q\left(\frac{n_b}{bt}\right) P(n_b, t). \quad (5.32)$$

Generally, one cannot solve this equation analytically. However, it is possible to discuss quantitatively the response function in the long time limit.

If the number of stable fixed points is finite, $\phi(t, t - \tau)/t$ converges to 0 as time increases. For simplicity, I consider a perturbation of delta-function type $\delta a \delta(t - \tau)$.

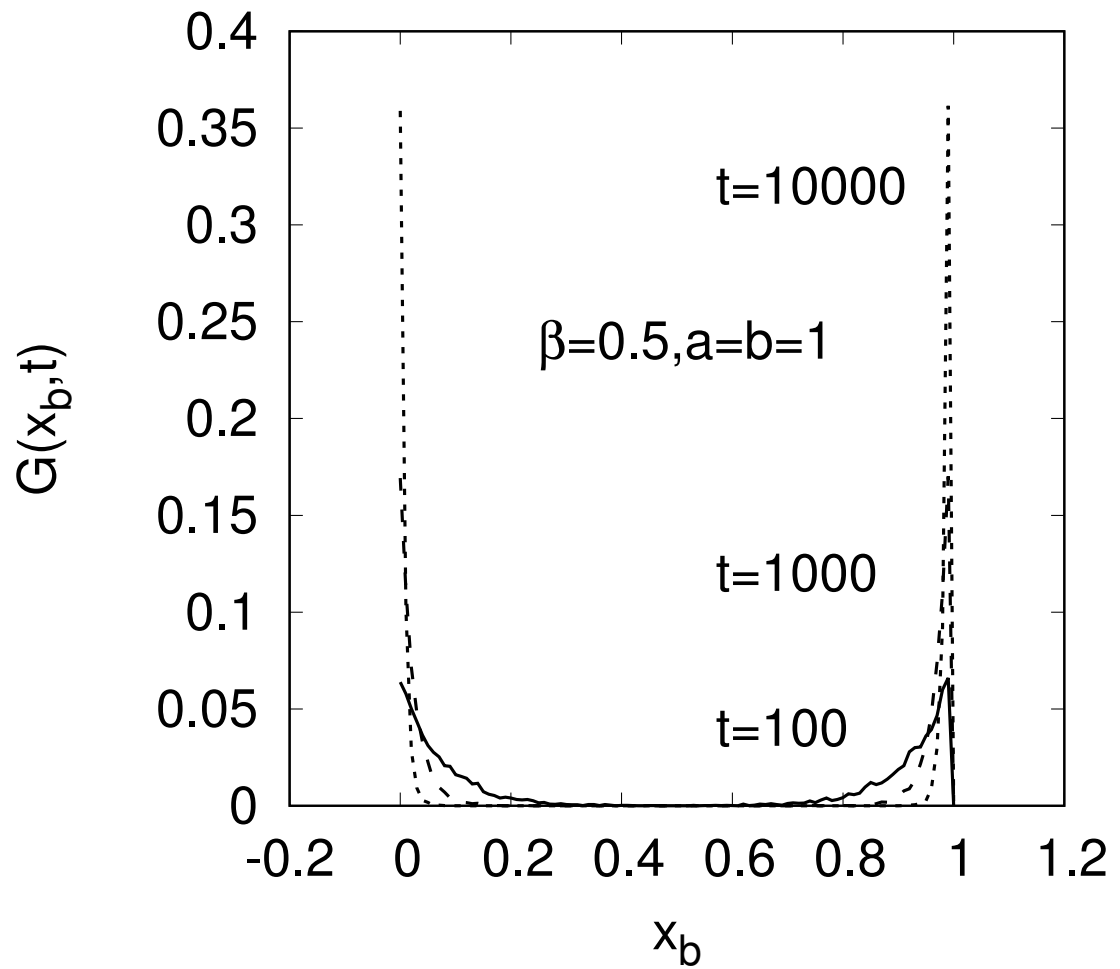


Figure 5.2: Distribution functions of black ball fraction $G(x_b, t)$ at $t = 100, 1000$, and 10000 for $\beta = 0.5$ and $a = b = 1$ in eq. (5.27).

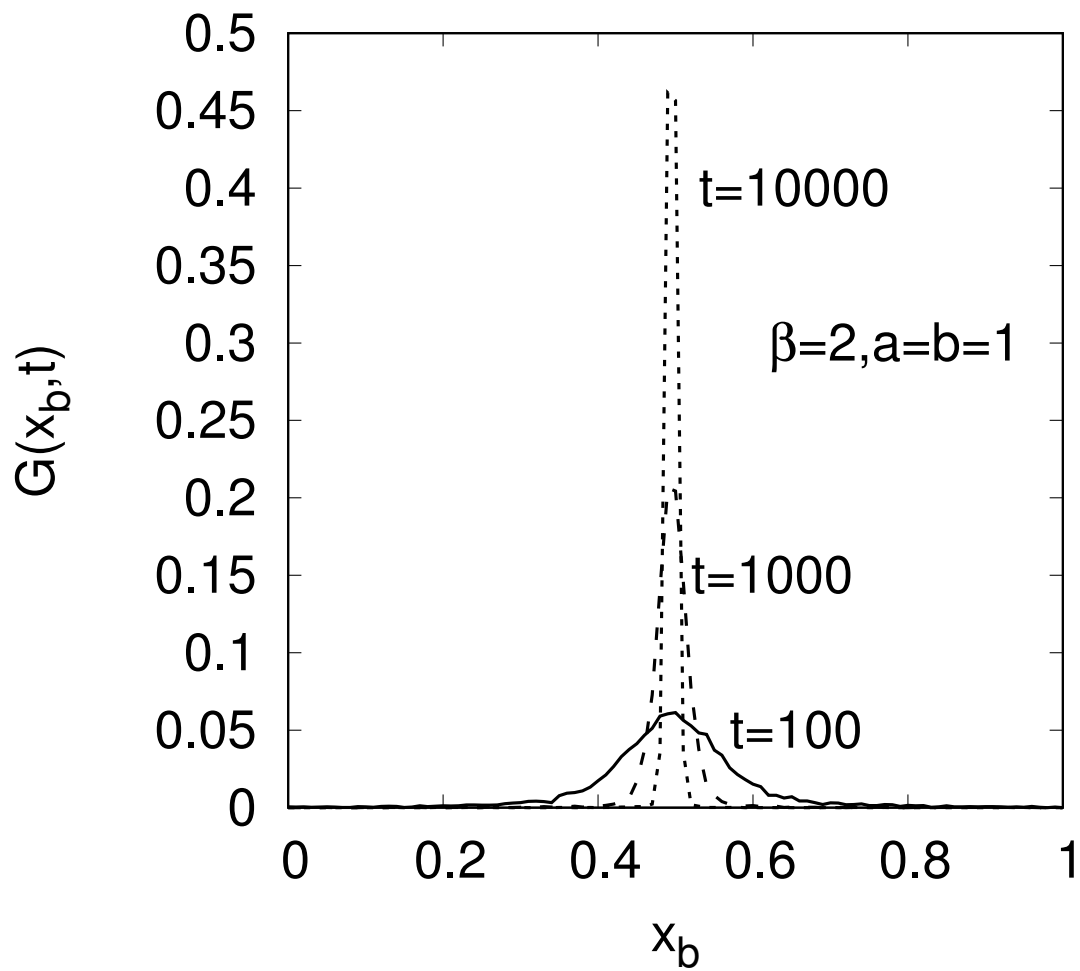


Figure 5.3: Distribution functions of the black ball fraction $G(x_b, t)$ at $t = 100, 1000$, and 10000 for $\beta = 2$ and $a = b = 1$ in eq. (5.27) when the probability of drawing the black ball $Q(x)$ is given by eq. (5.26).

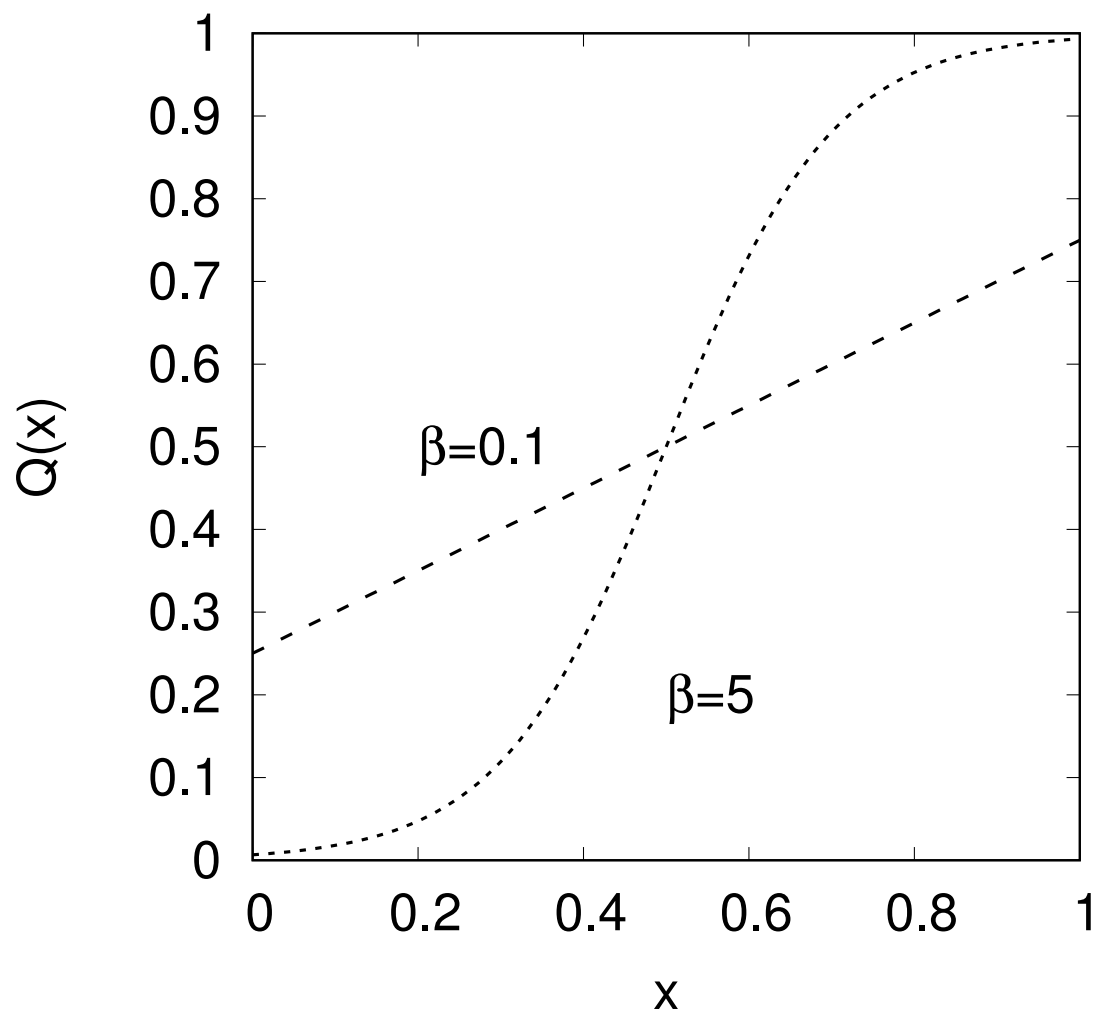


Figure 5.4: The x dependence of the probability of drawing the black ball $Q(x)$ given by eq. (5.28) for $\beta = 0.1$ and 5.

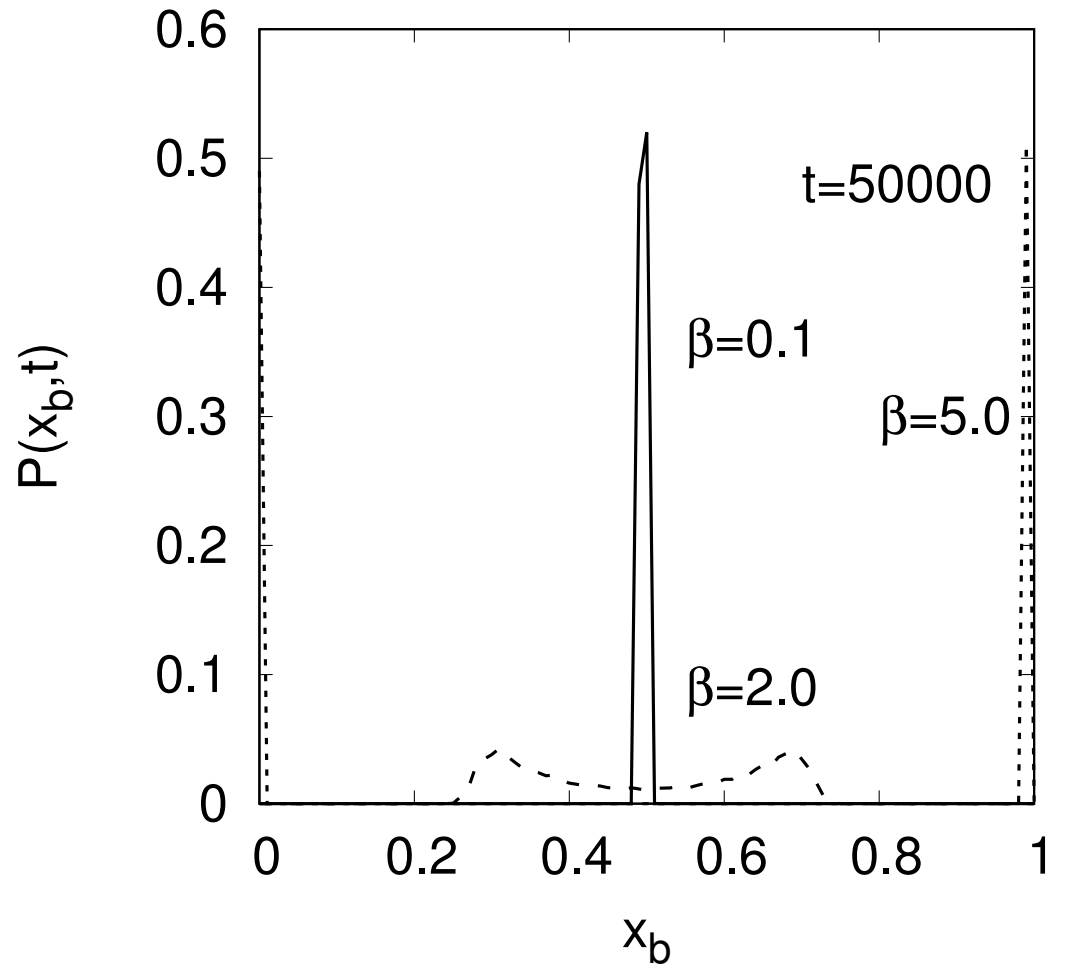


Figure 5.5: Distribution functions of the black ball fraction $G(x_b, t)$ at $t = 5000$ for $\beta = 0.1, 2$ and 5 and $a = b = 1$ in eq. (5.29). Here, the probability of drawing the black ball $Q(x)$ is given by eq. (5.28).

The fraction $x_b(t)$ calculated for the perturbed processes differs from $x_b^{n.p.}(t)$ at time $t \geq \tau$ where $x_b^{n.p.}(t)$ represents the fraction of black balls in the non-perturbed processes. However, for $t > \tau$, $x_b(t)$ is governed by the same dynamics of non-perturbation processes. Thus, $x_b(t)$ is attracted to a certain stable fixed point x_i^{st} . In the same way, $x_b^{n.p.}(t)$ converges to x_i^{st} in the long time limit. For this reason, $x_b(t) - x_b^{n.p.}(t) = (n_b(t) - n_b^{n.p.}(t))/bt$ decays to zero as $t \rightarrow \infty$.

The above discussion should hold generally. To confirm this result, I show the reduced response functions for two specific examples using analytical and numerical methods.

5.5.1 Example 3

The third example is represented by

$$Q(x) = \begin{cases} 0 & (x > 1/2) \\ 1/2 & (x = 1/2) \\ 1 & (x < 1/2), \end{cases} \quad (5.33)$$

$n_a(1) = n_b(1) = 1$, and $a = b$. Stable fixed points of the urn are 0 and 1. Since the number of the stable fixed points is two, this process is non-self-averaging.

The average numbers of black balls for non-perturbed and perturbed processes are

$$\langle n_b^{n.p.}(t) \rangle = 1 + \frac{a(t-1)}{2}, \quad (5.34)$$

and

$$\langle n_b(t) \rangle = 1 + \frac{a(t-1) + \delta a \Theta(t-\tau)}{2}, \quad (5.35)$$

respectively, where

$$\Theta(t) = \begin{cases} 0 & (t < 0) \\ 1 & (t \geq 0). \end{cases} \quad (5.36)$$

These results are exact because the stochastic effect is only at initial time $t = 1$. At the initial time, if one draws a black ball, only black balls are drawn after that because $Q(x_b) = 1$, and vice versa. The average of the response function is

$$\langle \phi(t, t-\tau) \rangle = \frac{\langle n_b(t) \rangle - \langle n_b^{n.p.}(t) \rangle}{\delta a}. \quad (5.37)$$

Consequently, one can obtain

$$\frac{\langle \phi(t, t-\tau) \rangle}{t} = \frac{\Theta(t-\tau)}{2t}. \quad (5.38)$$

In the long time limit, the average of the reduced response function decays to zero even if the process is non-self-averaging. Figure 5.6 shows the reduced response

functions in this case. The average is calculated by Monte Carlo simulations. This result supports eq. (5.38). This result differs from the result of the previous chapter. In the previous chapter, when self-averaging is violated, the average of the reduced response function does not decay to 0.

5.5.2 Example 4

Here, I consider the case

$$Q(x) = x^m \quad (5.39)$$

where m is a natural number larger than 1. I set $n_a(1) = n_b(1) = 1$, and $a = b$. Since a stable fixed point is 0, this process is self-averaging. Using the master equation (5.6), the averages of non-perturbed $n_b^{n.p.}(t)$ and perturbed $n_b(t)$ are described by

$$\frac{d\langle n_b^{n.p.}(t) \rangle}{dt} = a \frac{\langle (n_b^{n.p.}(t))^m \rangle}{a^m t^m} \simeq a \frac{\langle n_b^{n.p.}(t) \rangle^m}{a^m t^m}, \quad (5.40)$$

and

$$\frac{d\langle n_b(t) \rangle}{dt} = (a + \delta a \delta(t - \tau)) \frac{\langle (n_b(t))^m \rangle}{a^m t^m} \simeq (a + \delta a \delta(t - \tau)) \frac{\langle n_b(t) \rangle^m}{a^m t^m}, \quad (5.41)$$

respectively. The approximation $\langle n_b(t)^m \rangle \simeq \langle n_b(t) \rangle^m$ is valid for large t because of self-averaging.

Equations. (5.40) and (5.41) can be integrated by using separation of variables; thus

$$\langle n_b^{n.p.}(t) \rangle = \eta(t)^{1/(m-1)}, \quad (5.42)$$

and

$$\langle n_b(t) \rangle = \eta(t)^{1/(m-1)} \left\{ 1 + \frac{\delta a \Theta(t - \tau)}{(m-1)\eta(t)a^m \tau^m} \right\}, \quad (5.43)$$

where

$$\eta(t) = \frac{t^{m-1}}{a^{m-1}} + C \quad (5.44)$$

and C is a constant of integration. Using eq.(5.37) one can obtain

$$\frac{\langle \phi(t, t - \tau) \rangle}{t} = \frac{\eta(t)^{-m/(m-1)} \Theta(t - \tau)}{t(m-1)} \frac{1}{a^m \tau^m} \sim \frac{\Theta(t - \tau)}{t^{m-1}}. \quad (5.45)$$

I carried out Monte Carlo simulations for $m = 3$. Figure 5.7 shows that the average of the reduced response function goes to zero at $t \rightarrow \infty$. This behavior of the reduced response function agrees with eq. (5.45).

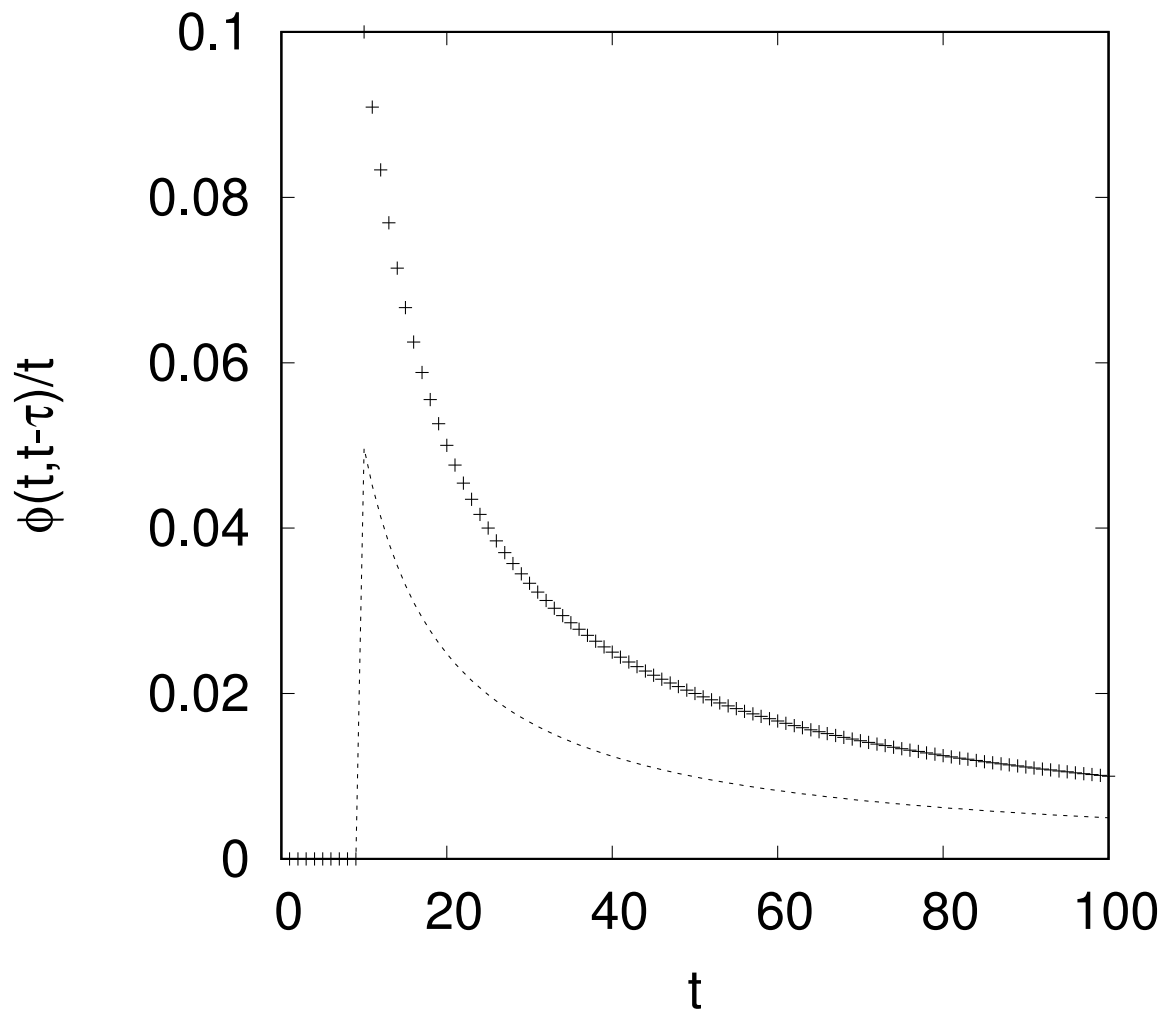


Figure 5.6: The reduced response functions $\phi(t, \tau)/t$ at $\tau = 10$, and $a = b = 1$ when the probability of drawing the black balls $Q(x)$ is given by eq. (5.33). The dashed curves are the average over 10^5 samples. Symbols represent the time series for a typical sample.

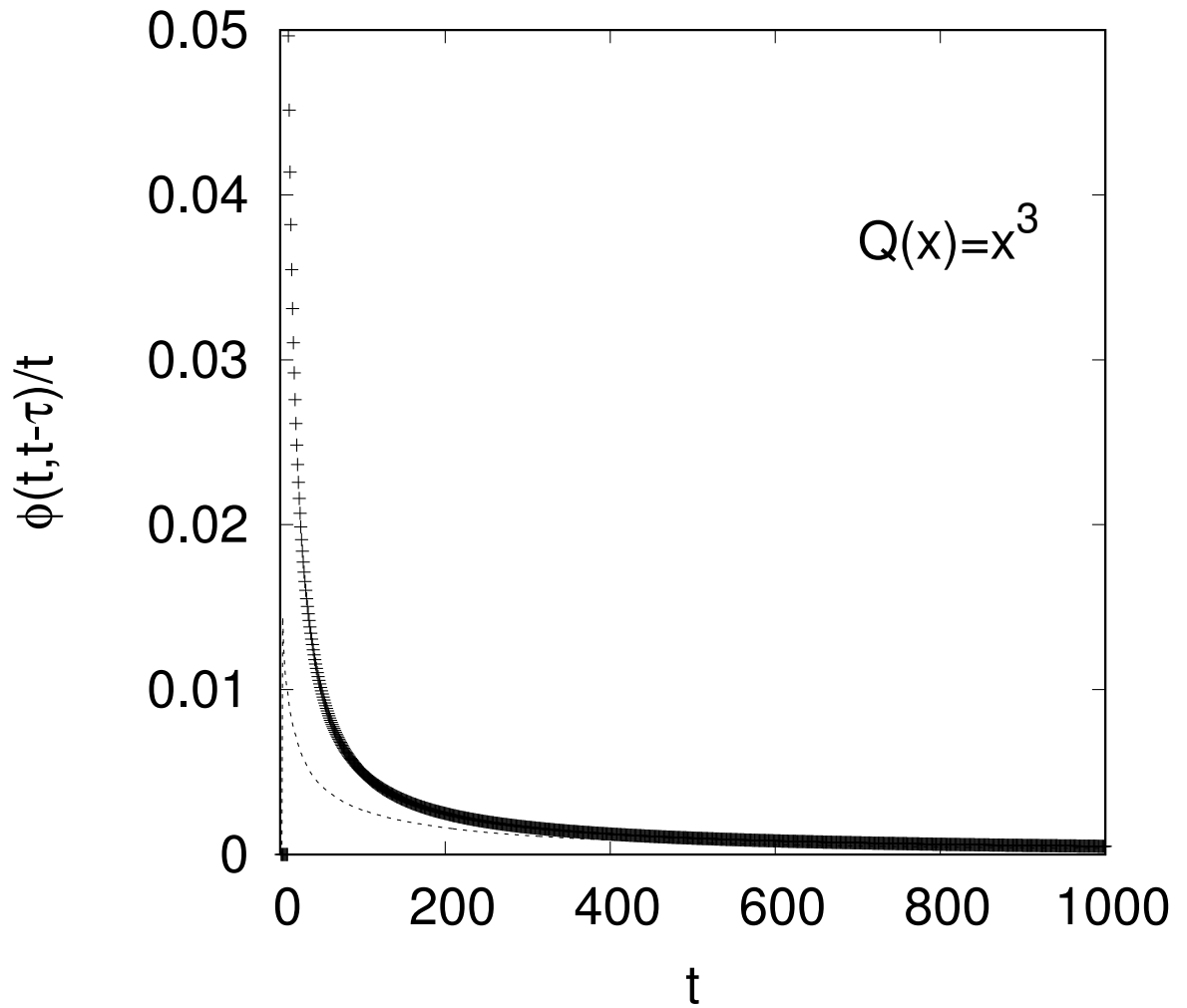


Figure 5.7: The reduced response function $\phi(t, \tau)/t$ for the probability of drawing the black balls $Q(x) = x^3$ with $\tau = 3$ and $a = b = 1$. The dashed curves are the average over 10^5 samples. Symbols represent the time series for a typical sample.

5.5.3 Classification of non-self-averaging

As shown by the last two examples, non-self-averaging does not correlate to behaviors of the reduced response function except for the case of the infinite number of $\{x_i^{st}\}$. If there is only one fixed point, this process is self-averaging. Applying perturbation to this process, I showed that the reduced response function $\phi(t, t - \tau)/t$ decays to zero in the long time limit (see Section 5.5.2). In the case, self-averaging processes correspond to the reduced response function decaying to 0 in the long time limit. However, when the number of stable fixed points is larger than 1, such correspondence does not exist. In this case, the reduced response function also converges to zero (see Section 5.5.1) although self-averaging is violated. Thus, the decay of $\phi(t, t - \tau)/t$ does not correlate to non-self-averaging.

In contrast, if the number of stable fixed points is infinite and the points constitute a dense set, this process is non-self-averaging. A typical example is linear Polya's urn process given by $Q(x) = x$ when $a = b$. In this case, the reduced response function does not go to 0 as time t increases.

From the above discussion, I find that there are two types of non-self-averaging stochastic processes. If the number of stable fixed points is infinite, this process is called strong non-self-averaging. In contrast, if the number of stable fixed points is finite, this process is called weak non-self-averaging. The behavior of $\phi(t, t - \tau)/t$ in the long time limit depend on whether the non-self-averaging is strong or weak. Therefore, I propose the following two classes. In the weak non-self-averaging processes, $\lim_{t \rightarrow \infty} \phi(t, t - \tau)/t = 0$. In the strong non-self-averaging process, $\lim_{t \rightarrow \infty} \phi(t, t - \tau)/t \neq 0$.

I conjecture that this difference reflects the functional forms of the distribution in the long time limit. For linear Polya's urn cases, the form of the distribution of n_b is flat-shaped (see fig. 4.1) when the process is strong non-self-averaging. However, for non-linear cases, the distribution of n_b has keen peaks (see fig. 5.3) since the process is weak non-self-averaging. If one observes only samples around a certain peak, it seems that the behavior of $n_b(t)$ is self-averaging. Therefore, the processes with an infinite number of stable fixed points give $\lim_{t \rightarrow \infty} \phi(t, t - \tau)/t \neq 0$, and have stronger non-self-averaging than other processes.

5.6 Conclusions

In this chapter, I introduced non-linear Polya's urn and analyzed the master equation. By the continuous master equation (5.6), I found that the equilibrium distribution $G_e(x_b)$ has some attractors x_i^{st} which satisfy $f(x_i) \stackrel{\text{def}}{=} aQ(x_i) - bx_i = 0$

and $f'(x_i) < 0$. Using these attractors, I obtained the exact distribution $G_e(x_b) = \sum_i \rho_i \delta(x_b - x_i^{st})$ in the long time limit. Moreover, I confirmed numerically the form of the distributions for specific examples. The results allow us to understand the condition of non-self-averaging unifiedly by the functional form of $Q(x_b)$ irrespective of whether the urn model is linear or non-linear. The non-self-averaging is also understood by the number of stable fixed points calculated by $Q(x_b)$. When the number of stable fixed points is infinite, the long-time behavior of $x_b(t)$ differs from that in the case of a finite number of stable fixed points. Thus, I define strong non-self-averaging by processes with an infinite number of stable fixed points, and weak non-self-averaging by processes with a finite number of stable fixed points.

The behavior of the reduced response function in the long time limit depends on whether non-self-averaging is strong or weak. The perturbation analysis shows that the reduced response function converges to 0 for weak non-self-averaging. Particularly, for specific forms of $Q(x_b)$, I derived the analytical form of the reduced response function and calculated these functions numerically. For linear Polya's urn, if self-averaging is strongly violated, the reduced response function does not decay to 0. In contrast, for non-linear Polya's urn, in the case of weak non-self-averaging, the reduced response function goes to 0.

However, if $Q(x_b)$ has a part equal to bx_b/a , the number of stable fixed points is infinite. Thus, the reduced response function does not decay to zero. In such cases, the process is non-self-averaging, because the number of stable fixed points is infinite. For this reason, I propose the following classification of non-self-averaging processes: (1) the processes where $\lim_{t \rightarrow \infty} \phi(t, t - \tau)/t \neq 0$ and (2) the processes where $\lim_{t \rightarrow \infty} \phi(t, t - \tau)/t = 0$.

Chapter 6

Conclusions

I analyzed Polya's urn that is a simple stochastic model to understand non-self-averaging, and Polya's urn model is known as a typical example exhibiting the behavior of non-self-averaging. So far the behaviors of Polya's urn model have been studied by many researchers. However, Polya's urn was not investigated in the time and frequency domains. Thus, to study the property of non-self-averaging in the time and frequency domains, I investigated the behavior of Polya's urn by using the perturbation analysis.

For linear Polya's urn, I showed the relation between the linear responses and non-self-averaging. If self-averaging is violated, several linear response functions do not decay to 0 in the long time limit. These functions are the average of the reduced response function, relaxation function, and complex admittance. These functions converge to 0 in the long time limit when the processes are self-averaging.

Next, I studied non-linear Polya's urn by using the perturbation analysis. From these results, I found that the relation between non-self-averaging and the relaxation of the reduced response function is not simple. When the number of stable fixed points is finite, and are larger than 1, the reduced response functions decay to 0 in non-self-averaging processes. However, if there are infinite stable fixed points, the average of the reduced response function does not decay.

Consequently, I propose the classification of non-self-averaging processes: (1) the strong class where the number of stable fixed points is infinite, and (2) the weak class where the number of stable fixed points is finite. When a non-self-averaging process belongs to the strong class, the average of the reduced response function does not decay to 0 in the long time limit. It goes to 0 in the long time limit for weak non-self-averaging processes. By classifying non-self-averaging processes in this way, I believe that it is possible to relate non-self-averaging with the linear response in general stochastic processes.

Acknowledgments

I would like to thank the following Professors for great help to me. Professor Takashi Odagaki has given me the occasion to study the present subject and insightful discussions. Professor Akira Yoshimori has guided me for a long time with many troubles. Professor Jun Matsui has advised and supported me for computations. Professor Jun-ichi Fukuda has helped me correct my thesis and given me valuable comments. Professor Hiizu Nakanishi has given me many comments.

Bibliography

- [1] M.V. Simkin, V.P. Roychowdhury, Phys. Rep, 502-1–35 (2011).
- [2] I. M. Lifshitz, Zh. Eksp. Teor. Fiz. 53, 743-758 (1968)
- [3] L. A. Pastur and M. V. Shcherbina, J Stat. Phys. 62 1-19 (1991).
- [4] A. Aharony and A. B. Harris. Phys. Rev. Lett. 77, 3700–3703 (1996).
- [5] A Malakis and N. G. Fytas, Phys. Rev. E 73, 016109 (2006)
- [6] P. L. Krapivsky, I. Grosse, E. Ben-Naim, Phys. Rev E 61, R993(R) (2000)
- [7] M. Kawasaki, T. Odagaki and K. Kehr, Phys. Rev. B 61, 5839–5842 (2000)
- [8] M. Kawasaki, T. Odagaki and K. Kehr, Phys. Rev. B 67, 134203-1–16 (2003).
- [9] M. Aoki, UCLA Economics Online Papers No 375 (2006).
- [10] F. Eggenberger and G. Polya, Z. Ang. Math. Mech. 3, 279–289 (1923).
- [11] M. Aoki and H. Yoshikawa, Economics Discussion Papers No. 2007-49 (2012).
- [12] N. Aoki and H. Yoshikawa, RITEI Discussion Paper Series, 07-E-057 (2007).
- [13] H. Yamato and M. Sibuya, Bulletin of Informatics and Cybernetics, 32, 1-10 (2000).
- [14] M. Hoppe, J. Math. Biol. 20, 91-94 (1984)
- [15] P. Flajolet, J. Gabarró and H. Pekar. The Annals of Probability 33,1200–1233 (2005).
- [16] C. Godreche and J. M Luck, J,Phys. Condens. Matter 14, 1601 (2002)
- [17] S. Mori, M. Hisakado and T. Takahashi, Phys. Rev. E 86, 026109-1–10 (2012).
- [18] S. Janson, Stoch. Proc. Appl. 110 177-245 (2004)

- [19] L. A. N. Amaral, P. Gopikrishnan, V. Plerou, H. E. Stanley, *Physica A* 299, 127-136 (2001).
- [20] A. Bottazi and A. Secchi, *Physica A*, 324, 213-219 (2002)
- [21] W. Feller, “An Introduction to Probability Theory and Its Applications”, Vol. 1, Ed. 3, Wiley (1968)
- [22] A. Bagchi and A. K. Pal, *Siam J Algebra Discr* 6(3) 394-405 (1985).
- [23] H.A. Simon, *Biometrika*, 42 425 (1955).
- [24] R. T. Smythe, *Stoch Proc Appl* 65 115-137 (1996)
- [25] S. Noguchi, A. Yoshimori, J. Fukuda and T. Odagaki, submitted.
- [26] S. Balaji and H. M. Mahmoud, *Ann. Inst. Stat. Math.* 58, 171–185(2006)
- [27] W. B. Arthur, Y. M. Ermoliev, Y. M. Kaniovskii *Proc of the Int. Conf. on Stoch. Optim*, 287-300 (1984)